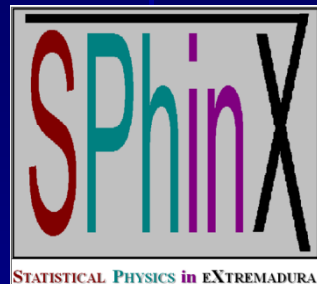


Penetrable-particle fluids as models of ultra-soft colloids

Andrés Santos

University of Extremadura, Badajoz, Spain



Collaborators:

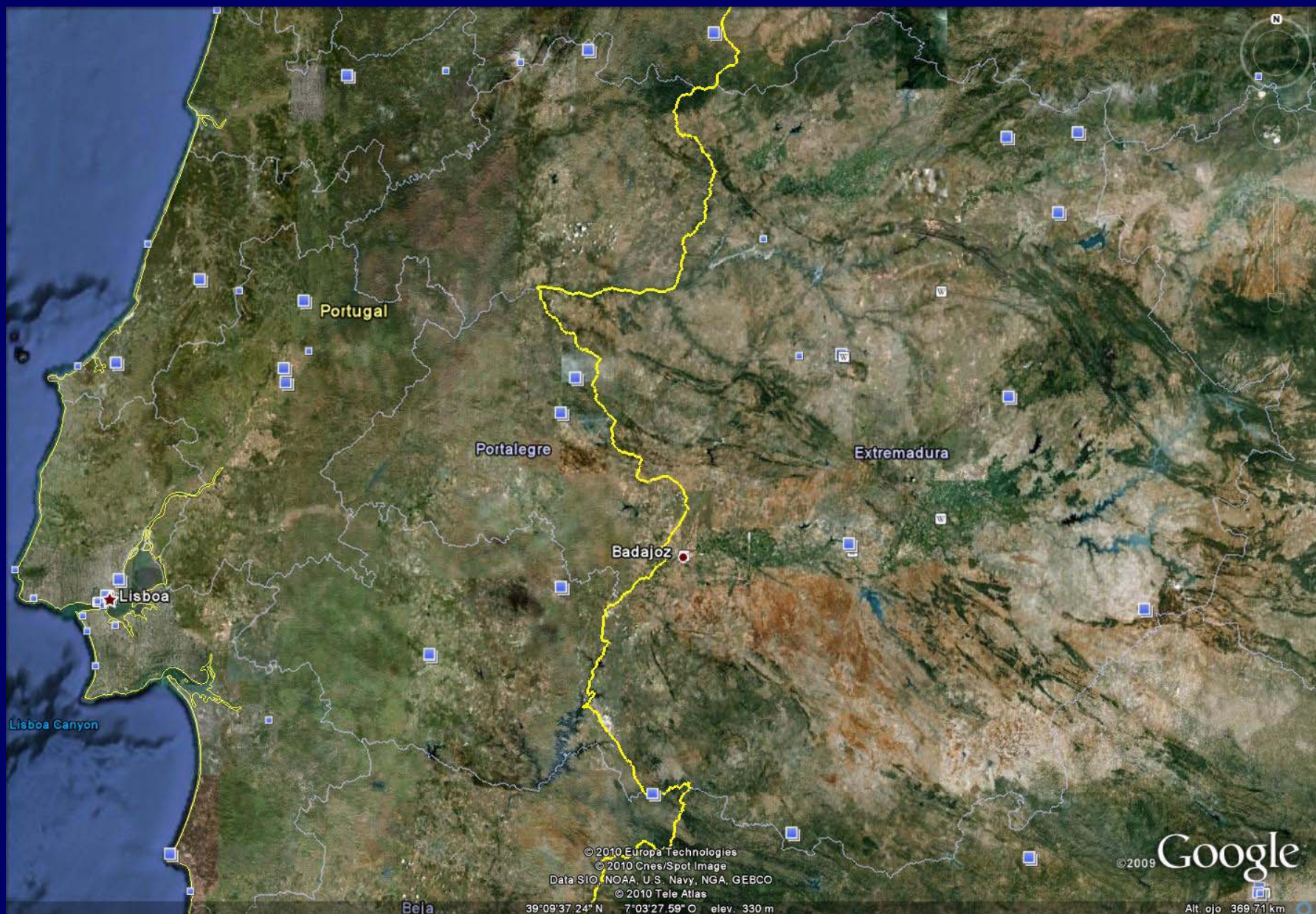
Luis Acedo (Valencia, Spain)

Alexandr Malijevský (Prague, Czech Rep.)

Santos Bravo Yuste (Badajoz, Spain)

Riccardo Fantoni (Venice, Italy)

Achille Giacometti (Venice, Italy)



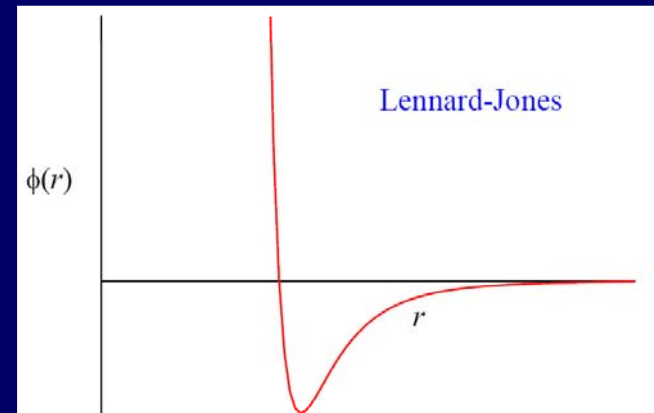
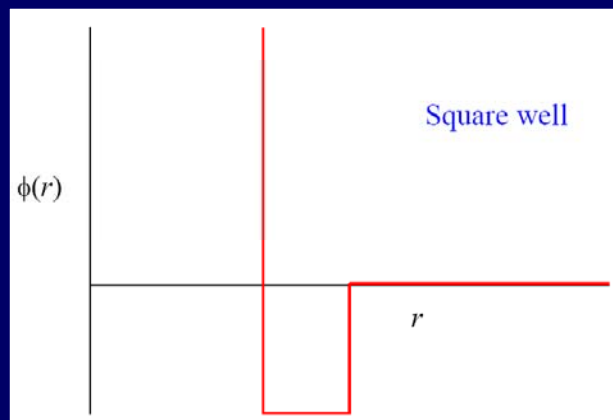
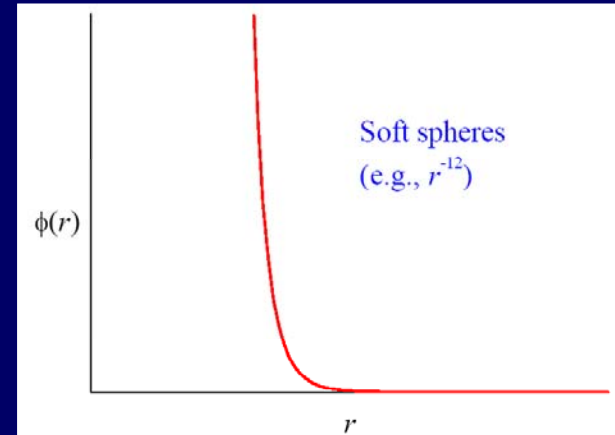
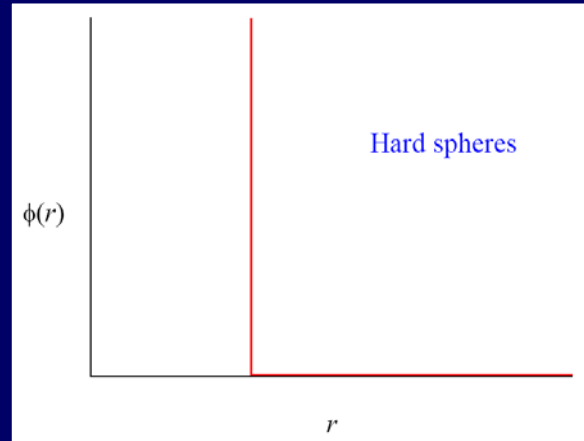
Outline

- Effective interactions in colloidal dispersions. The penetrable-sphere (PS) model.
- Some basic concepts of statistical mechanics of equilibrium liquids.
- Exact properties of the PS fluid. Low-density limit. High-temperature, high-density limit.
- The high-penetrability and low-penetrability approximations.
- The penetrable-square-well (PSW) model.
- Transport properties of the PS model.
- Conclusions.

Outline

- Effective interactions in colloidal dispersions. The penetrable-sphere (PS) model.
- Some basic concepts of statistical mechanics of equilibrium liquids.
- Exact properties of the PS fluid. Low-density limit. High-temperature, high-density limit.
- The high-penetrability and low-penetrability approximations.
- The penetrable-square-well (PSW) model.
- Transport properties of the PS model.
- Conclusions.

Traditionally, equilibrium statistical mechanics has been applied to systems made of particles interacting via *unbounded* potentials, e.g.,



In fact, unbounded potentials are useful models to represent the interactions not only in *atomic* systems ($\sigma \approx 1 \text{ \AA} = 0.1 \text{ nm}$), but also in some *colloidal* dispersions ($1\text{nm} < \sigma < 1 \mu\text{m}$).

For instance, the effective interaction between two sterically stabilized colloidal particles is essentially of hard-sphere (HS) type, perhaps with a short-range attraction (depletion effects).

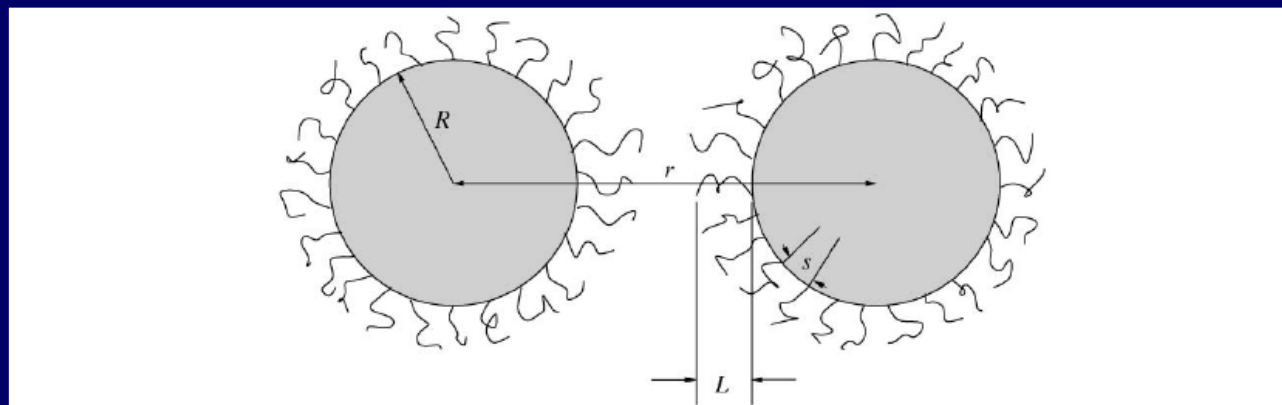


Fig. 4. Two sterically stabilized colloidal particles, each being covered with a polymeric brush whose height is L . The distance between neighboring anchored chains is denoted by s .

C.N. Likos / Physics Reports 348 (2001) 267–439

On the other hand, the effective interaction for *star polymers* in good solvents is ultrasoft, logarithmically diverging for short distances.

C.N. Likos / Physics Reports 348 (2001) 267–439

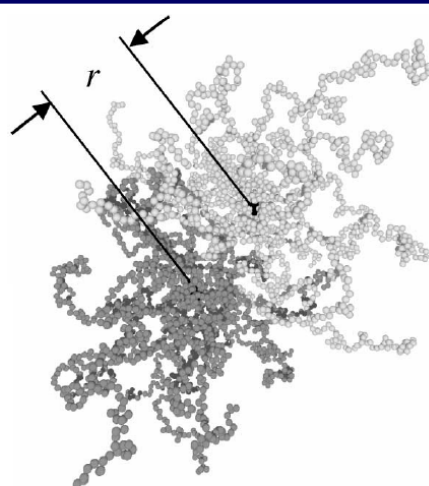


Fig. 42. Typical configuration for two stars with $f = 30$ and $N = 50$, as obtained from a simulation of Ref. [78], with r denoting the distance between their centers. (Courtesy of Ar[1].)

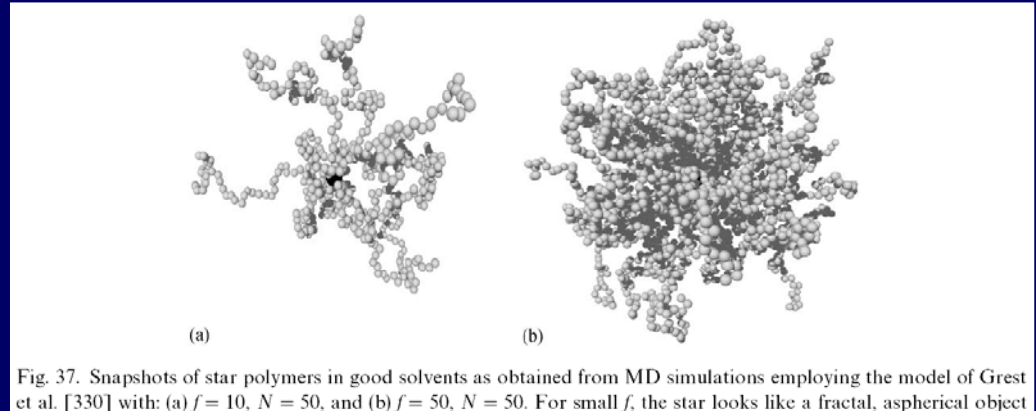


Fig. 37. Snapshots of star polymers in good solvents as obtained from MD simulations employing the model of Grest et al. [330] with: (a) $f = 10$, $N = 50$, and (b) $f = 50$, $N = 50$. For small f , the star looks like a fractal, aspherical object whereas for large f it resembles a spherical, colloidal particle. (Taken from Ref. [331].)

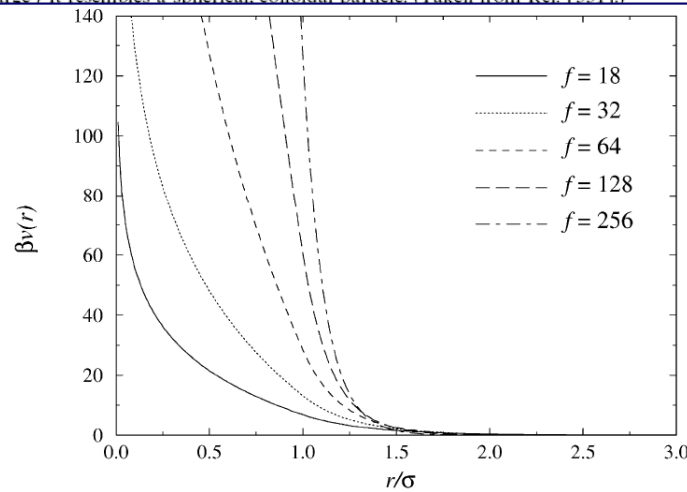


Fig. 40. The effective star-star potential of Eq. (5.57) for a number of different f -values. Notice that the potential becomes harder with increasing f , tending eventually to a HS interaction for $f \rightarrow \infty$.

What about dilute solutions of *polymer chains* in good solvents?

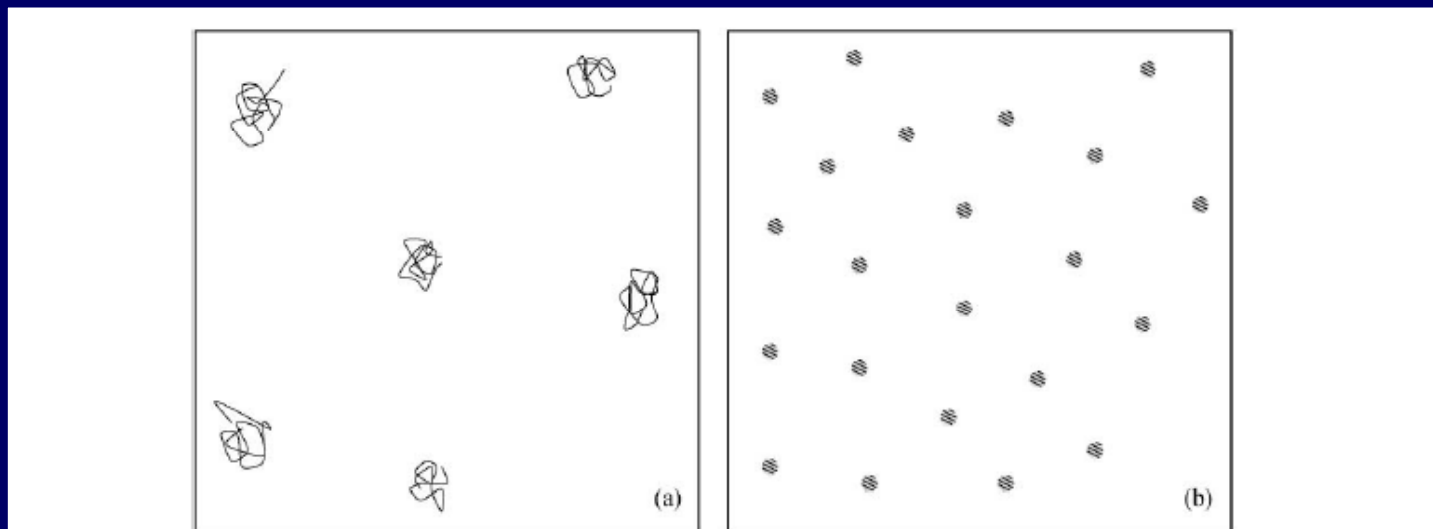


Fig. 13. A dilute polymer solution observed through two different microscopes. In (a) the microscope can resolve details above the monomer length whereas in (b) the microscope can only resolve details above the size of the chain. As a result, all length scales in (b) appear reduced with respect to those in (a) and the objects which appear as flexible chains in (a) show up as “point particles” in (b). Note that the field of view in (b) includes many more particles than in (a).

C.N. Likos / Physics Reports 348 (2001) 267–439

Two polymer chains can “sit on top of each other”

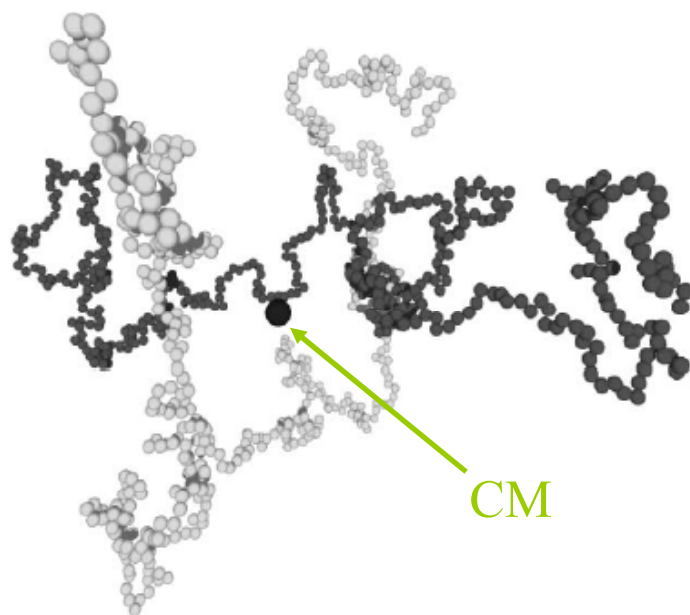
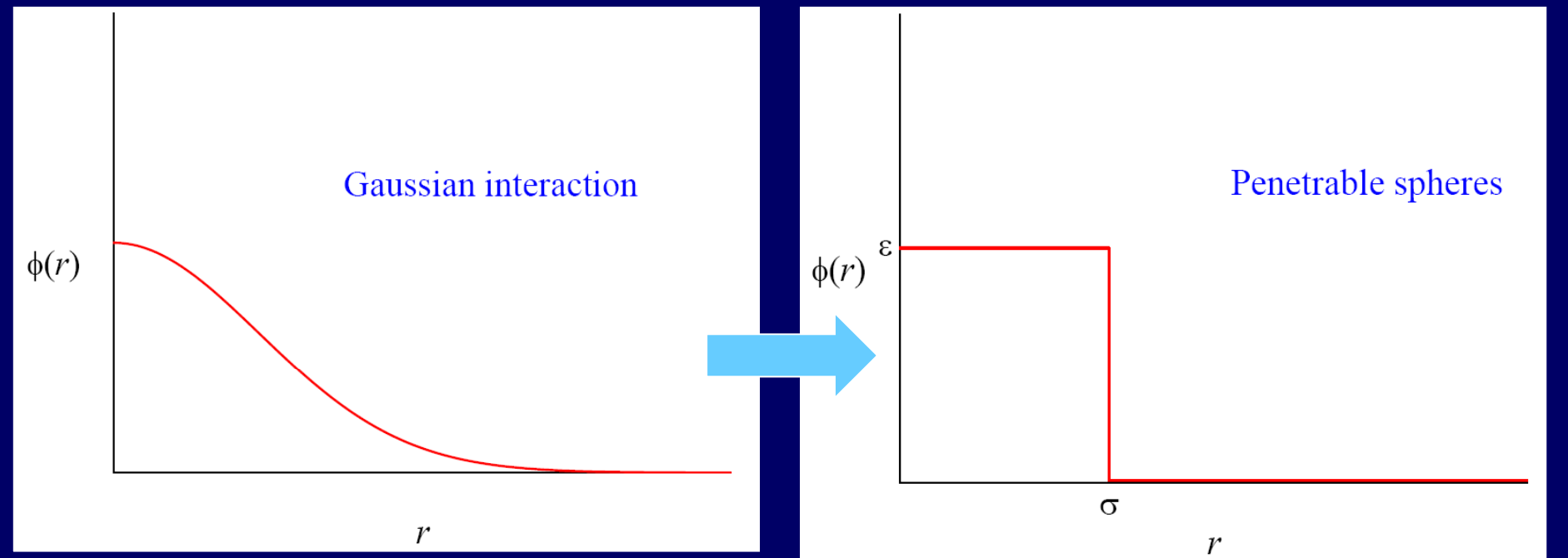


Fig. 14. A snapshot from a simulation involving two self-avoiding polymers. In this configuration, the centers of mass of the two chains (denoted by the big sphere) coincide, without violation of the excluded-volume conditions. (Courtesy of Arben Jusufi.)

C.N. Likos / Physics Reports 348 (2001) 267–439

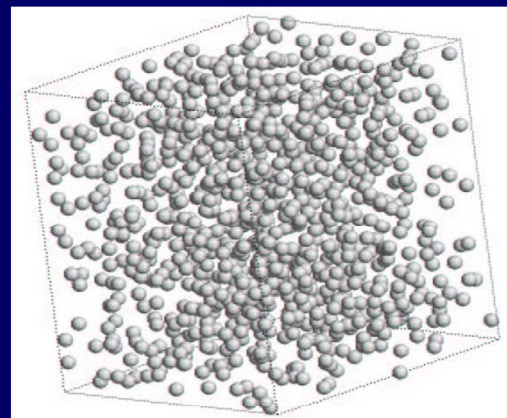
Effective interaction between two polymer chains in a good solvent: *Bounded* potentials, e.g.,



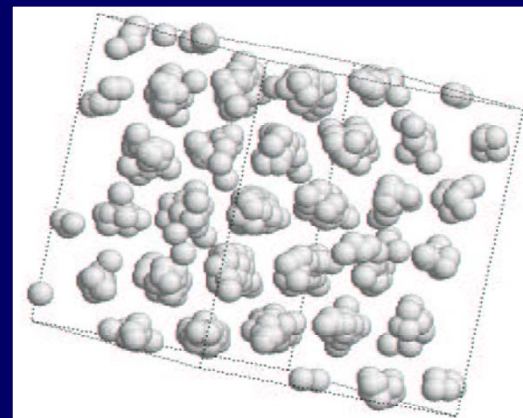
MC simulations (Bianca Mladek, Technische Universität Wien, 2003)

$T^*=0.5$

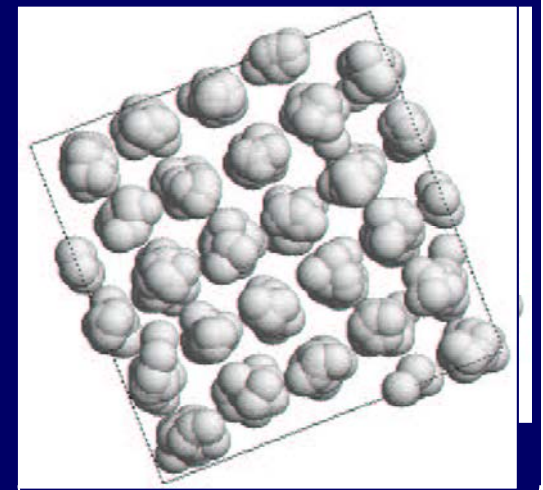
$\rho\sigma^3=0.5$



$\rho\sigma^3=3.5$



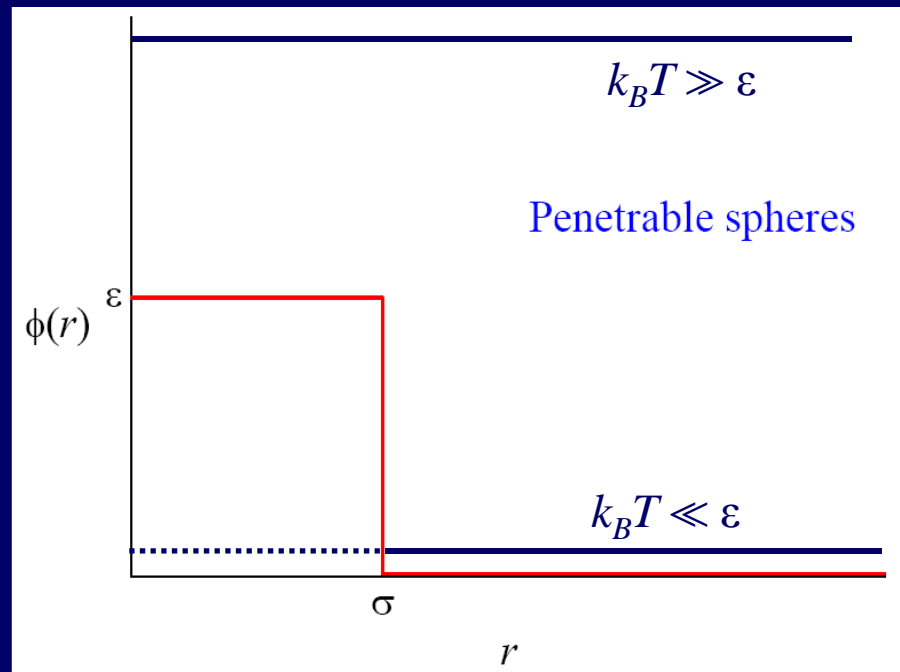
$\rho\sigma^3=4.0$



fluid

crystal

Aim: To obtain *analytical* approximations for the (equilibrium) structural and thermophysical properties of a PS fluid and compare with MC simulations



$$T^* \equiv k_B T / \varepsilon$$

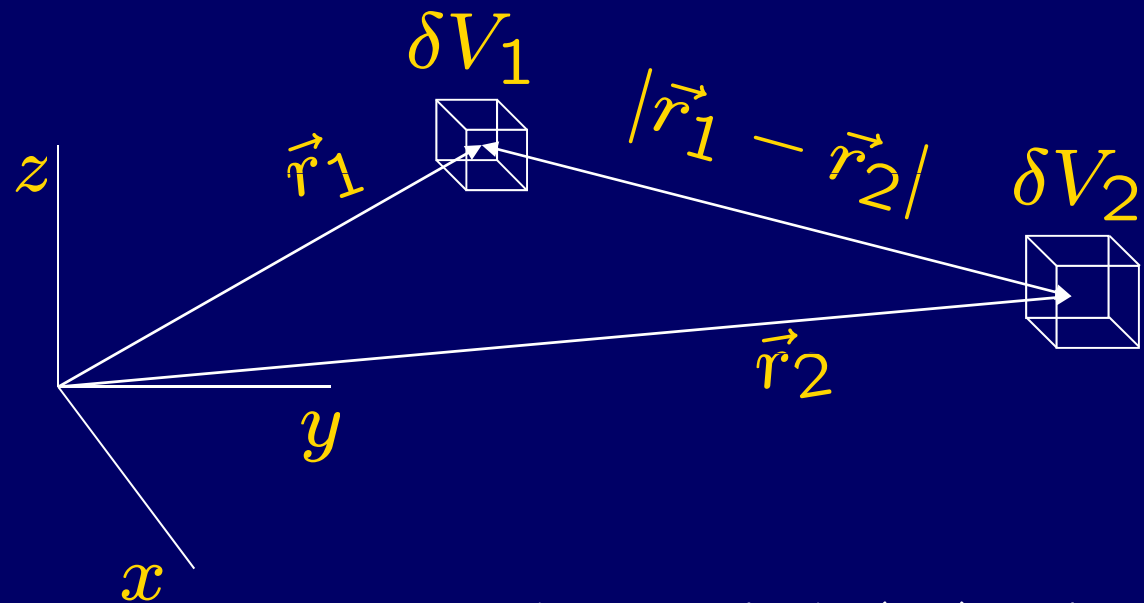
$T^* \rightarrow \infty$: ideal gas
 $T^* \rightarrow 0$: HS fluid

Outline

- Effective interactions in colloidal dispersions. The penetrable-sphere (PS) model.
- Some basic concepts of statistical mechanics of equilibrium liquids.
- Exact properties of the PS fluid. Low-density limit. High-temperature, high-density limit.
- The high-penetrability and low-penetrability approximations.
- The penetrable-square-well (PSW) model.
- Transport properties of the PS model.
- Conclusions.

Pair correlation function or radial distribution function, $g(r)$

$$N_{\text{pairs}}(\vec{r}_1, \vec{r}_2) = \left(\frac{N}{V} \delta V_1 \right) \left(\frac{N}{V} \delta V_2 \right) g(|\vec{r}_1 - \vec{r}_2|)$$



Quantities related with $g(r)$

$y(r) = e^{\phi(r)/k_B T} g(r)$: cavity function

$h(r) = g(r) - 1$: total correlation function

$c(r)$: direct correlation function

$\tilde{c}(k) = \frac{\tilde{h}(k)}{1 + \rho \tilde{h}(k)}$: Ornstein–Zernike relation

$S(k) = 1 + \rho \tilde{h}(k)$: structure factor

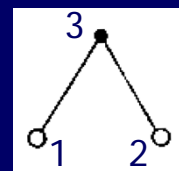
Expansion of the radial distribution function in powers of density:

$$y(r) \equiv e^{\phi(r)/k_B T} g(r) = 1 + \sum_{n=1}^{\infty} \frac{\rho^n}{n!} y_n(r)$$

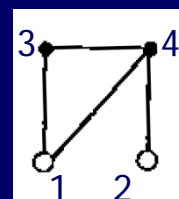
$$\begin{aligned} y_1(r) &= \text{Diagram of a triangle with two open circles at the vertices and one at the top vertex} \\ y_2(r) &= 2 \text{Diagram of a square with two open circles at the top-left and bottom-left vertices} + 4 \text{Diagram of a square with two open circles at the top-left and top-right vertices} + \text{Diagram of a square with two open circles at the top-left and bottom-right vertices} + \text{Diagram of a square with two open circles at the bottom-left and bottom-right vertices} \\ y_3(r) &= 6 \text{Diagram of a triangle with two open circles at the bottom-left and bottom-right vertices} + 6 \text{Diagram of a triangle with two open circles at the top-left and top-right vertices} + 12 \text{Diagram of a triangle with two open circles at the top-left and bottom-right vertices} + 12 \text{Diagram of a triangle with two open circles at the top-right and bottom-right vertices} \\ &\quad + 6 \text{Diagram of a square with two open circles at the top-left and bottom-left vertices} + 12 \text{Diagram of a square with two open circles at the top-left and top-right vertices} + 12 \text{Diagram of a square with two open circles at the top-right and bottom-right vertices} + 6 \text{Diagram of a square with two open circles at the top-left and bottom-right vertices} \\ &\quad + 6 \text{Diagram of a triangle with two open circles at the top-left and top-right vertices} + 6 \text{Diagram of a triangle with two open circles at the top-left and bottom-right vertices} + 6 \text{Diagram of a triangle with two open circles at the top-right and bottom-right vertices} + 6 \text{Diagram of a square with two open circles at the top-left and top-right vertices} \\ &\quad + 12 \text{Diagram of a square with two open circles at the top-left and bottom-left vertices} + \text{Diagram of a square with two open circles at the top-left and bottom-right vertices} + 3 \text{Diagram of a square with two open circles at the top-right and bottom-right vertices} + 12 \text{Diagram of a triangle with three open circles at the vertices} \\ &\quad + 12 \text{Diagram of a square with three open circles at the vertices} + 3 \text{Diagram of a triangle with three open circles at the vertices} + 3 \text{Diagram of a square with three open circles at the vertices} + 6 \text{Diagram of a triangle with three open circles at the vertices} \\ &\quad + 6 \text{Diagram of a square with three open circles at the vertices} + 6 \text{Diagram of a triangle with three open circles at the vertices} + 3 \text{Diagram of a square with three open circles at the vertices} + \text{Diagram of a triangle with four open circles at the vertices} \end{aligned}$$

$$f(r) = e^{-\phi(r)/k_B T} - 1$$

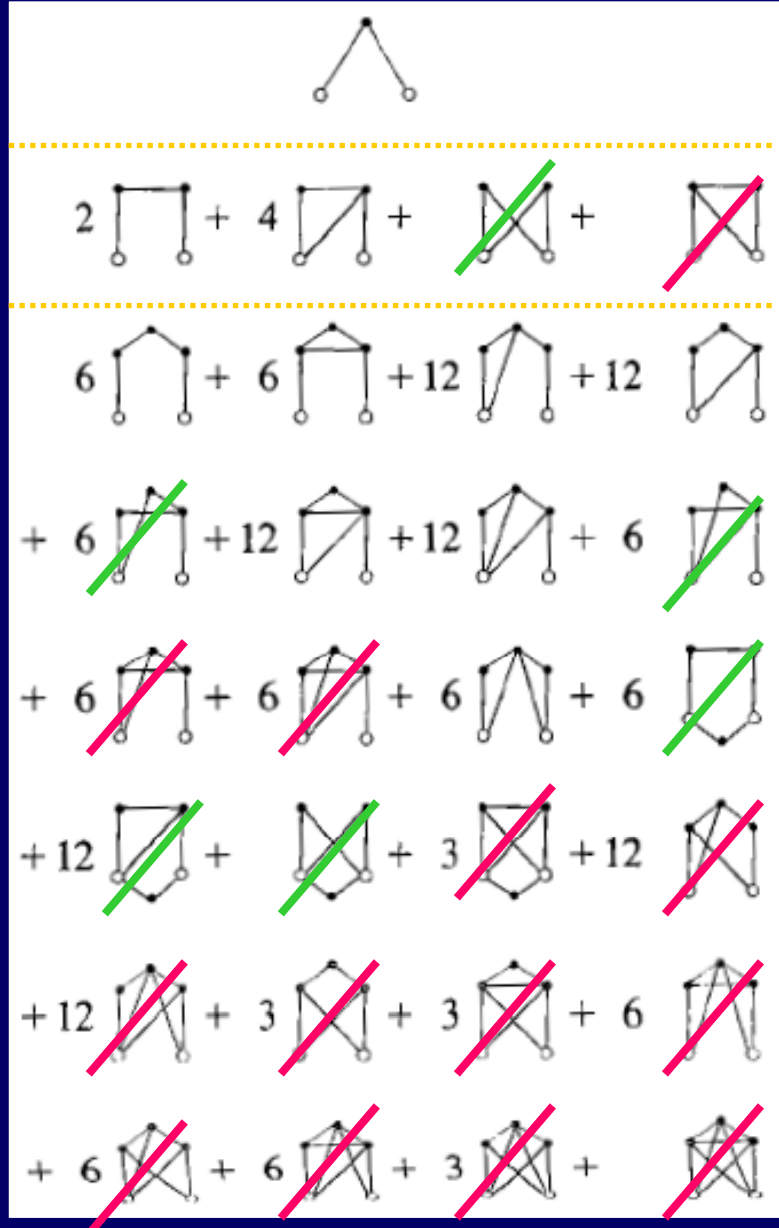
Mayer function



$$= \int d\mathbf{r}_3 f(r_{13}) f(r_{23})$$



$$\begin{aligned} &= \int d\mathbf{r}_3 \int d\mathbf{r}_4 f(r_{13}) f(r_{34}) \\ &\quad \times f(r_{24}) f(r_{14}) \end{aligned}$$



HNC closure:

$$c(r) = g(r) - 1 - \ln y(r)$$

"Elementary" diagrams neglected

Percus–Yevick (PY) closure:

$$c(r) = f(r)y(r)$$

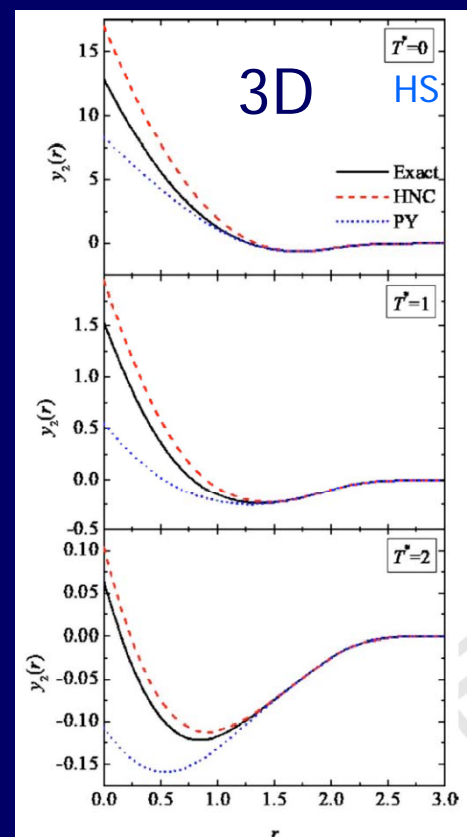
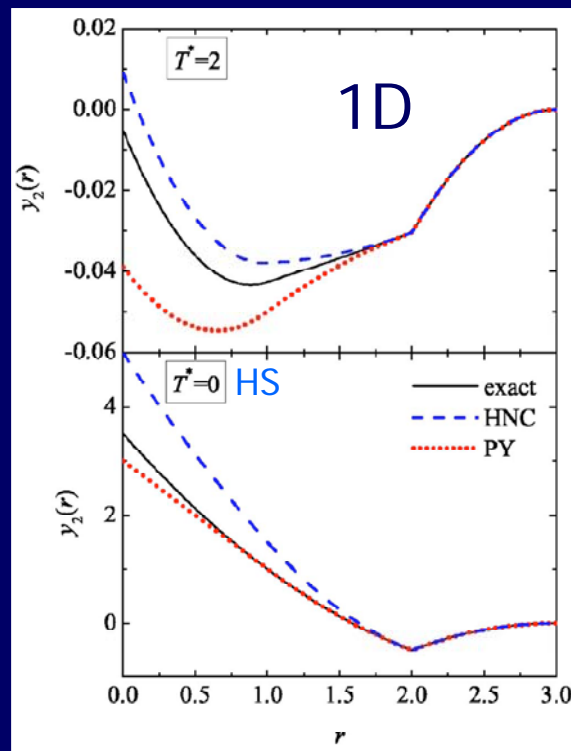
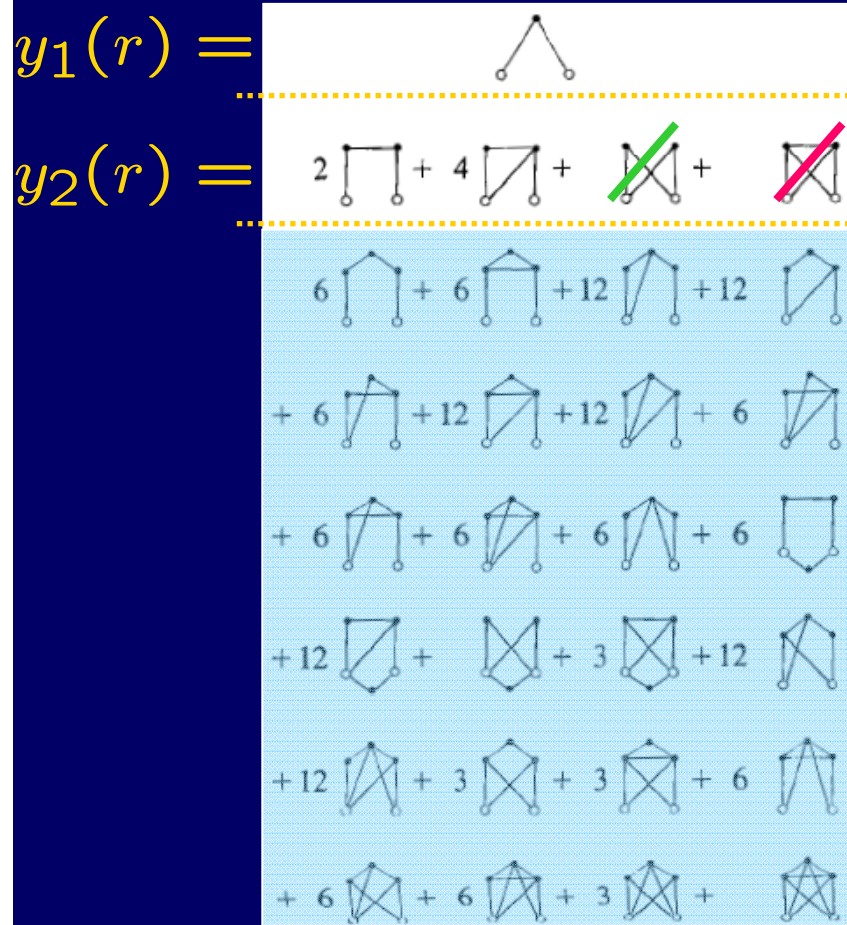
"Elementary" and "Bundle" diagrams neglected

Outline

- Effective interactions in colloidal dispersions. The penetrable-sphere (PS) model.
- Some basic concepts of statistical mechanics of equilibrium liquids.
- Exact properties of the PS fluid. Low-density limit. High-temperature, high-density limit.
- The high-penetrability and low-penetrability approximations.
- The penetrable-square-well (PSW) model.
- Transport properties of the PS model.
- Conclusions.

Exact behavior to second order in density

$$y(r) \equiv e^{\phi(r)/k_B T} g(r) = 1 + \sum_{n=1}^{\infty} \frac{\rho^n}{n!} y_n(r)$$



Al. Malijevský and A. Santos

J. Chem. Phys. **124**, 074508 (2006)

PHYSICAL REVIEW E **75**, 021201 (2007)

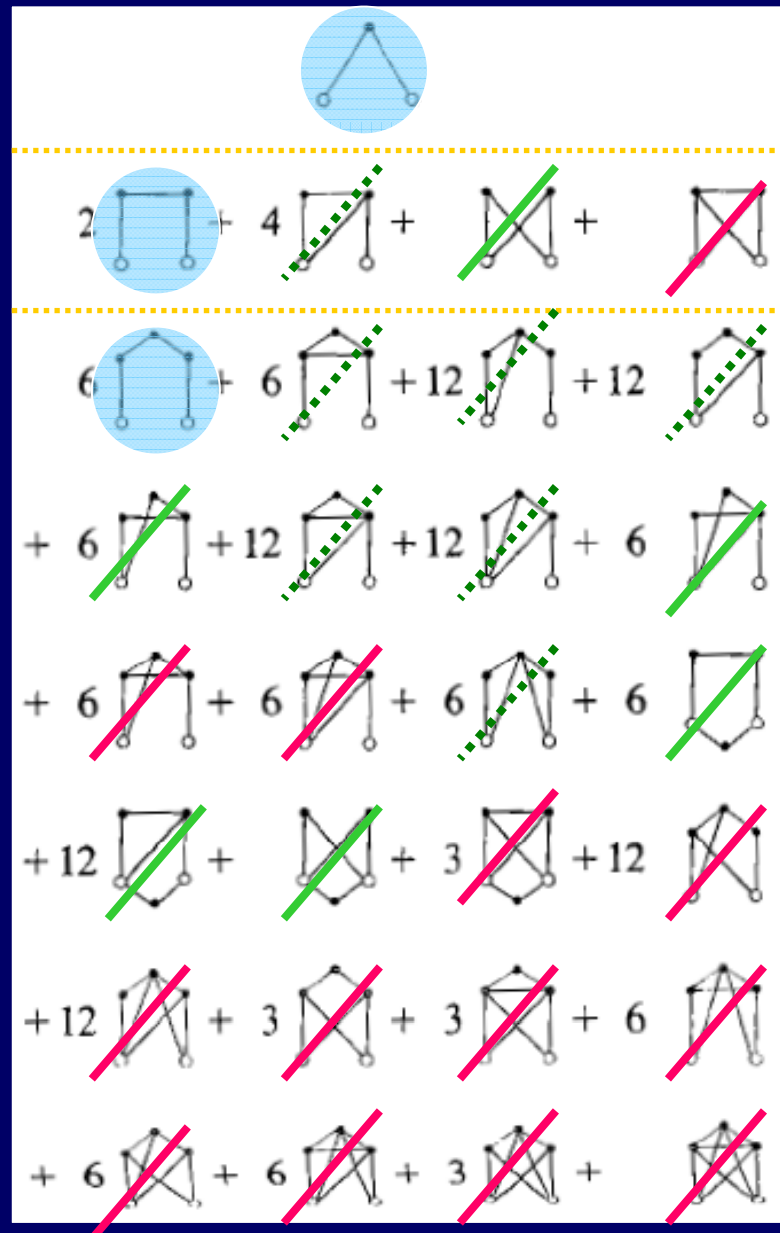
Mayer function of the PS model

$$f_{\text{PS}}(r) = xf_{\text{HS}}(r), \boxed{x \equiv 1 - e^{-1/T^*}}$$

“Opacity” (or “impenetrability”) parameter

$$f_{\text{HS}}(r) = \begin{cases} -1, & r < \sigma \\ 0, & r > \sigma \end{cases}$$

The PS model in the high-temperature, high-density limit



$$T^* \rightarrow \infty \Rightarrow x \approx T^{*-1} \rightarrow 0$$

$$\rho \rightarrow \infty, \hat{\rho} \equiv \rho x = \text{finite}$$

Only “chain” diagrams survive!

The PS model in the high-temperature, high-density limit (mean-field theory)

[L. Acedo & A.S., Phys. Lett. A **323**, 427 (2004)]

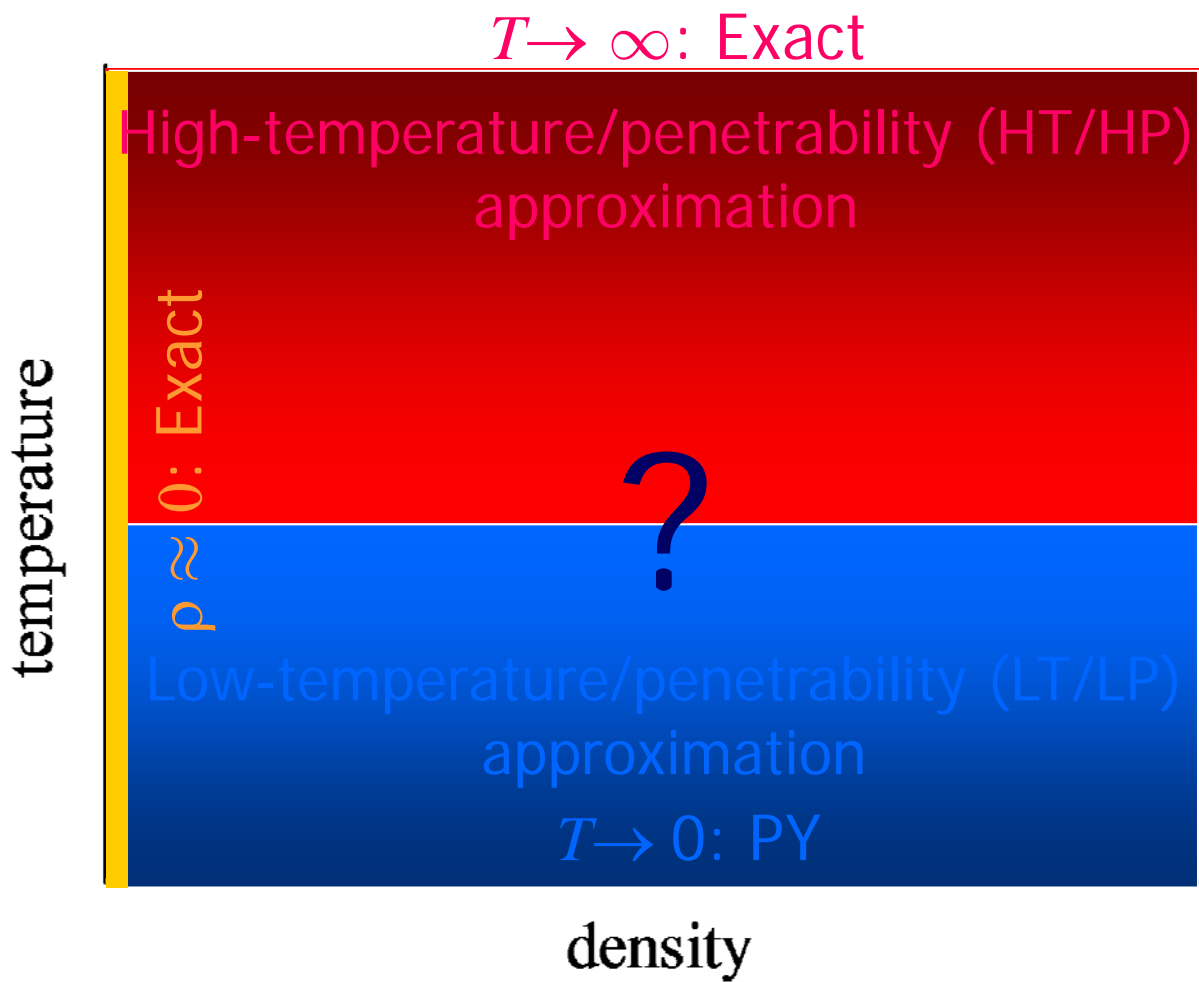
$$\lim_{\substack{x \rightarrow 0 \\ \rho \rightarrow \infty \\ \hat{\rho} = \rho x}} y(r) = 1 + x \sum_{n=1}^{\infty} \hat{\rho}^n \circ \bullet \cdots \bullet \circ$$
$$= 1 + x w(r)$$

$$\tilde{w}(k) = \hat{\rho} \frac{[\tilde{f}_{HS}(k)]^2}{1 - \hat{\rho} \tilde{f}_{HS}(k)}$$

$$\lim_{\substack{x \rightarrow 0 \\ \rho \rightarrow \infty \\ \hat{\rho} = \rho x}} S(k) = \frac{1}{1 - \hat{\rho} \tilde{f}_{HS}(k)}, \quad \lim_{\substack{x \rightarrow 0 \\ \rho \rightarrow \infty \\ \hat{\rho} = \rho x}} c(r) = x f_{HS}(r)$$

Outline

- Effective interactions in colloidal dispersions. The penetrable-sphere (PS) model.
- Some basic concepts of statistical mechanics of equilibrium liquids.
- Exact properties of the PS fluid. Low-density limit. High-temperature, high-density limit.
- The high-penetrability and low-penetrability approximations.
- The penetrable-square-well (PSW) model.
- Transport properties of the PS model.
- Conclusions.



High-temperature (HT/HP) approximation

[Al. Malijevský, S. B. Yuste, A.S., Phys. Rev. E **76**, 021504 (2007)]

$$\lim_{\substack{x \rightarrow 0 \\ \rho \rightarrow \infty \\ \hat{\rho} = \rho x}} y(r) = 1 + xw(r), \quad x \equiv 1 - e^{-1/T^*}$$

$$\boxed{\text{HT: } y(r) = 1 + xw(r)e^{xw(r)}}$$

$$g(r) = \begin{cases} (1 - x)y(r), & r < \sigma \\ y(r), & r > \sigma \end{cases}$$

Low-temperature (LT/LP) approximation

[Al. Malijevský, S. B. Yuste, A.S., Phys. Rev. E **76**, 021504 (2007)]

$$g(r) = \frac{e^{Q(r)\Theta(1-r)}}{r} \sum_{n=0}^{\infty} f_n(r-n)\Theta(r-n)$$

$$Q(r) = (r-1)[A + B(r+2)(r-1) + Cr(r-1)]$$

$$f_n(r) = -\mathcal{L}^{-1} \left\{ \frac{t}{12\eta} \frac{(1 + S_1 t + S_2 t^2 + S_3 t^3) (L_0 + L_1 t)^n}{(L_0 + S_1 t + S_2 t^2 + S_3 t^3)^{n+1}} \right\}$$

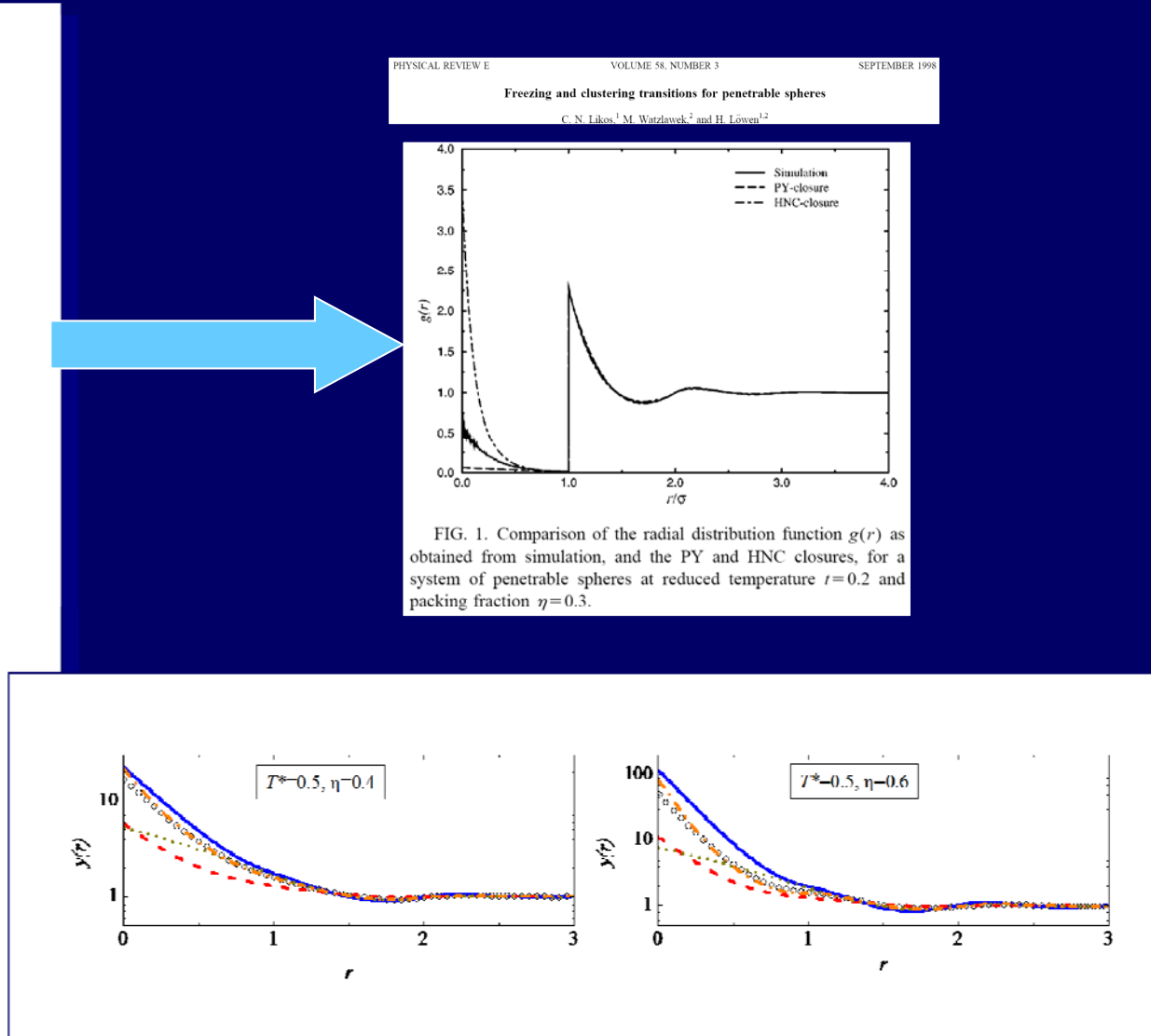
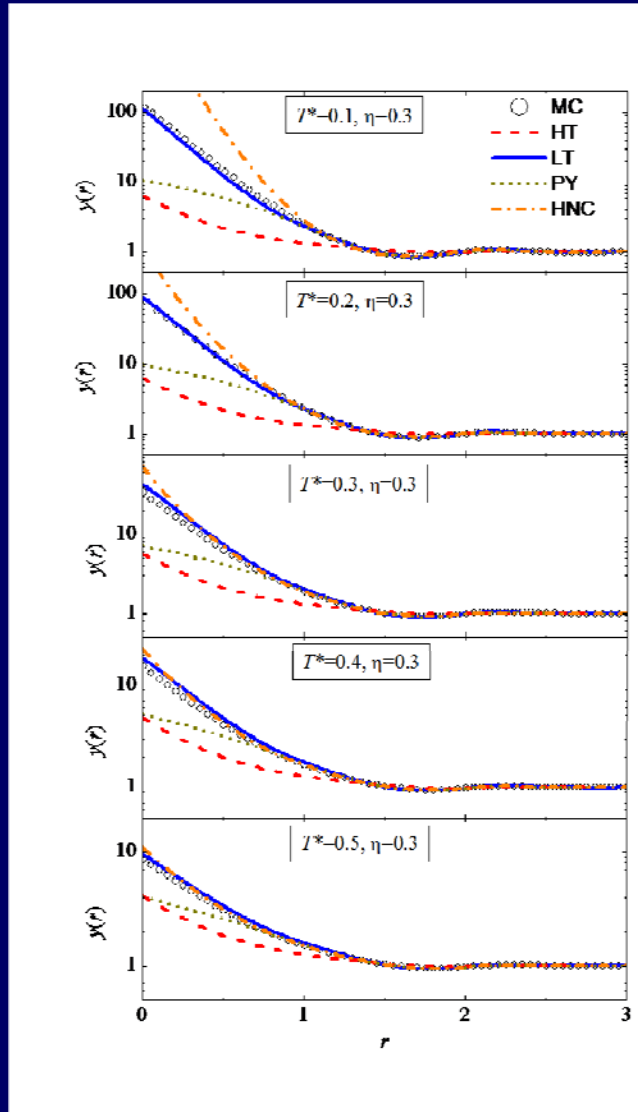
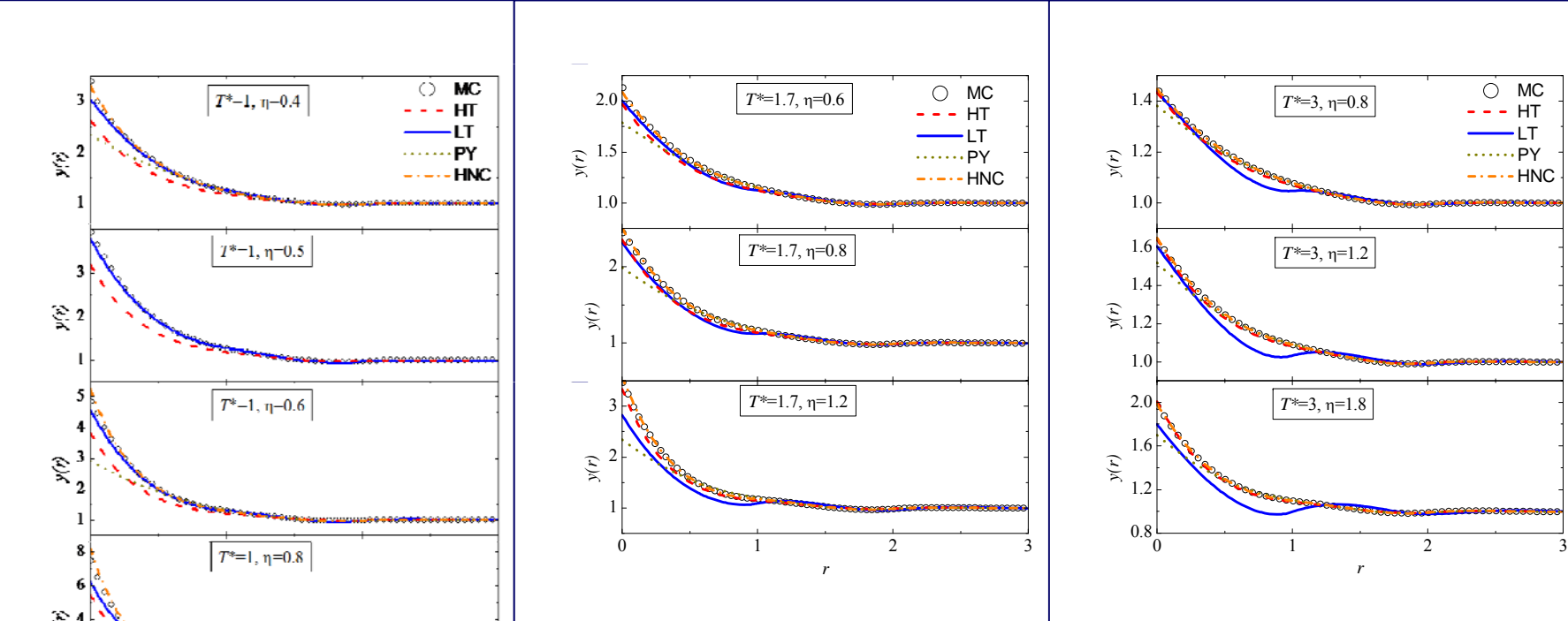
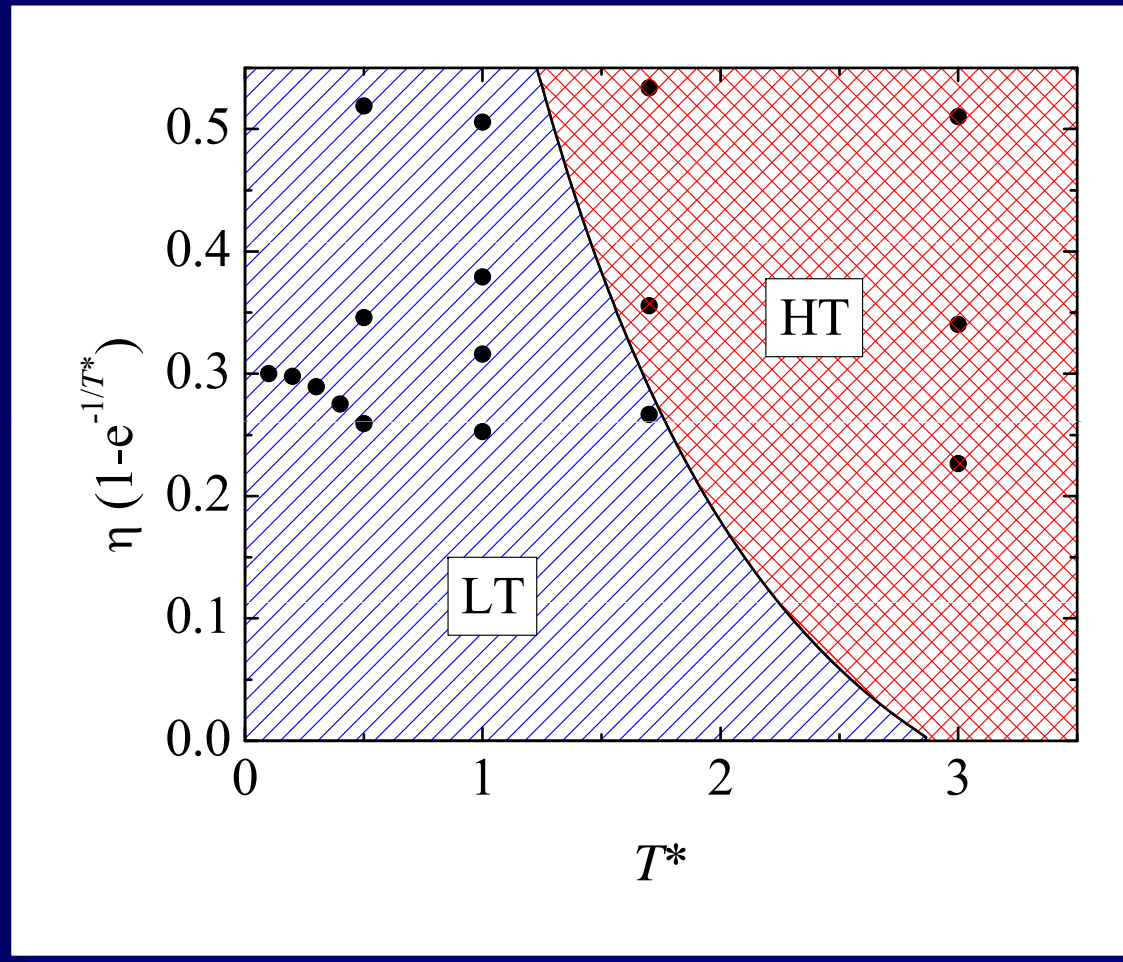


FIG. 1. Comparison of the radial distribution function $g(r)$ as obtained from simulation, and the PY and HNC closures, for a system of penetrable spheres at reduced temperature $T=0.2$ and packing fraction $\eta=0.3$.



“Domains” of the HT and LT approximations

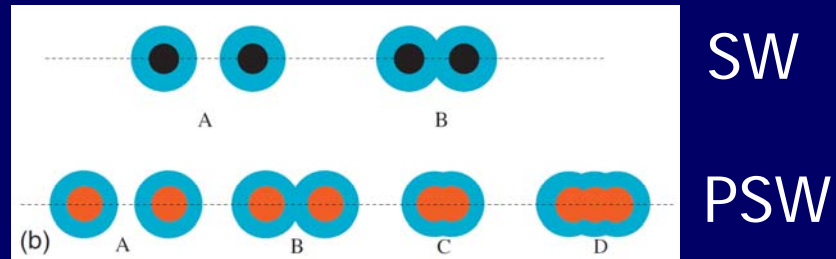
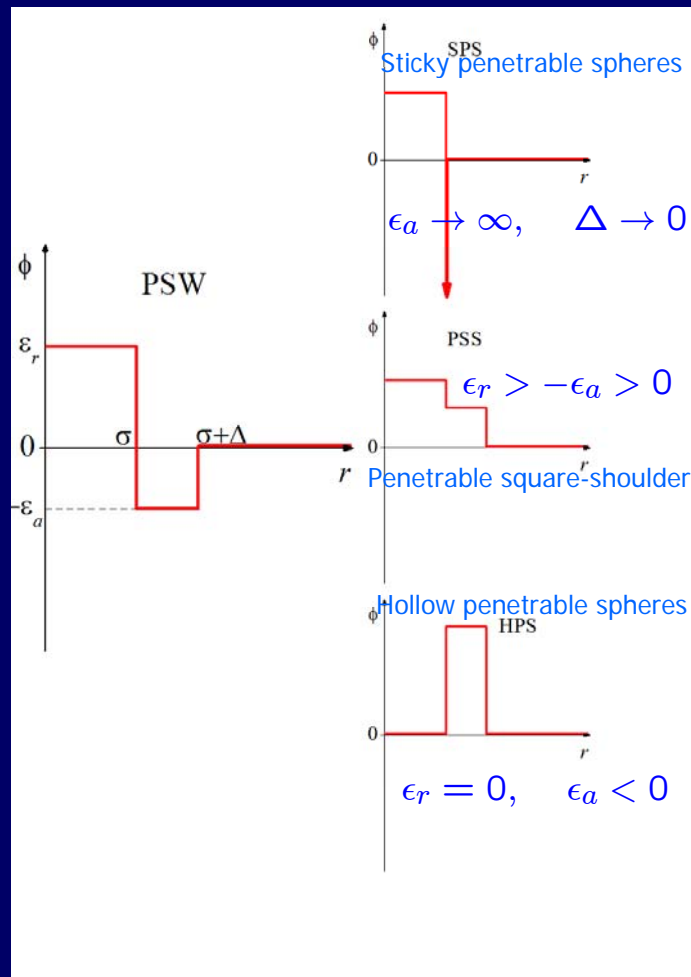


Skip PSW?

Outline

- Effective interactions in colloidal dispersions. The penetrable-sphere (PS) model.
- Some basic concepts of statistical mechanics of equilibrium liquids.
- Exact properties of the PS fluid. Low-density limit. High-temperature, high-density limit.
- The high-penetrability and low-penetrability approximations.
- The penetrable-square-well (PSW) model.
- Transport properties of the PS model.
- Conclusions.

The Penetrable-Square-Well (PSW) Model



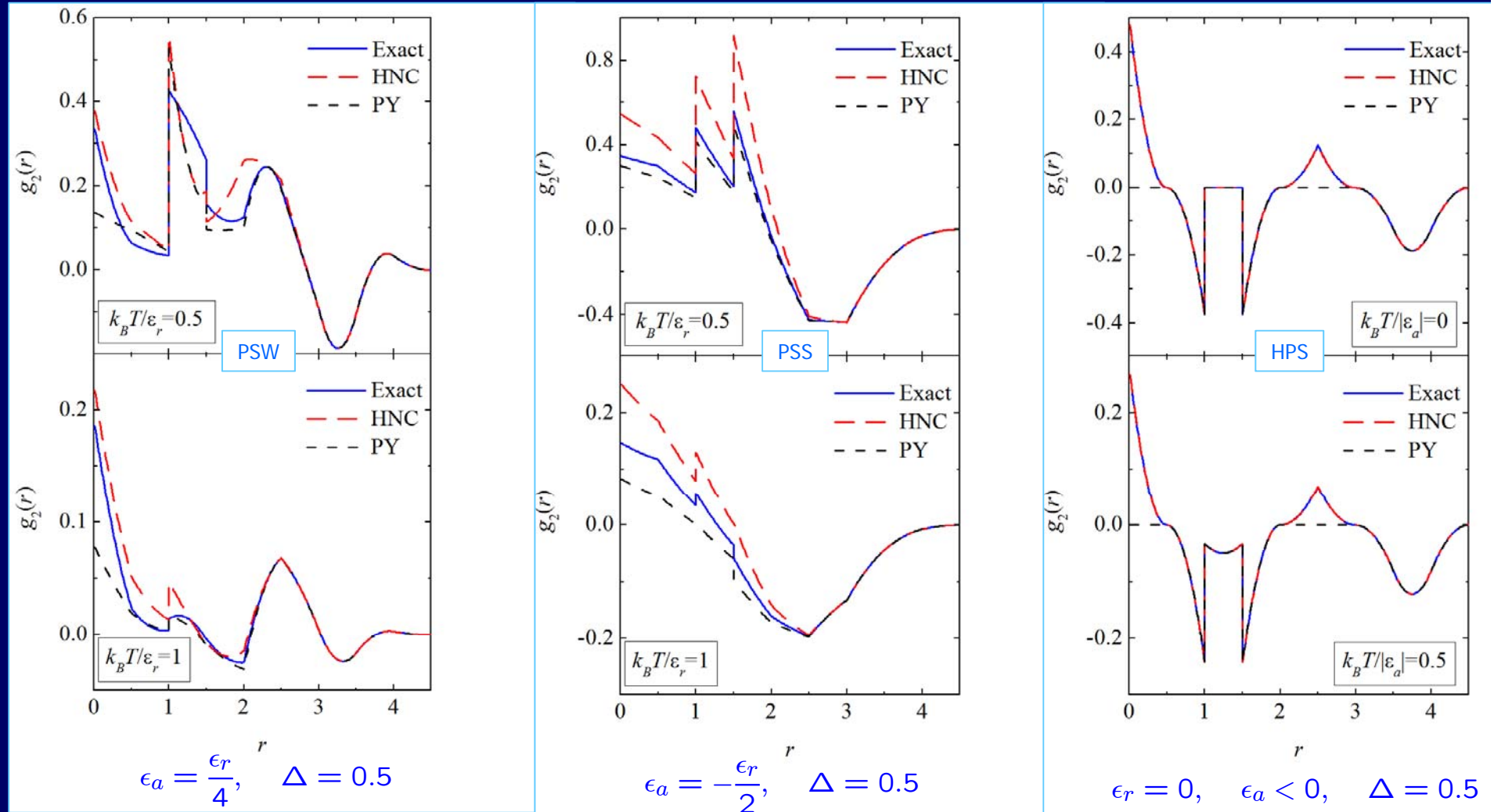
Necessary condition for thermodynamic stability:

$$\epsilon_r > 2\epsilon_a$$

[A.S. R. Fantoni, A. Giacometti, Phys. Rev. E **77**, 051206 (2008)]

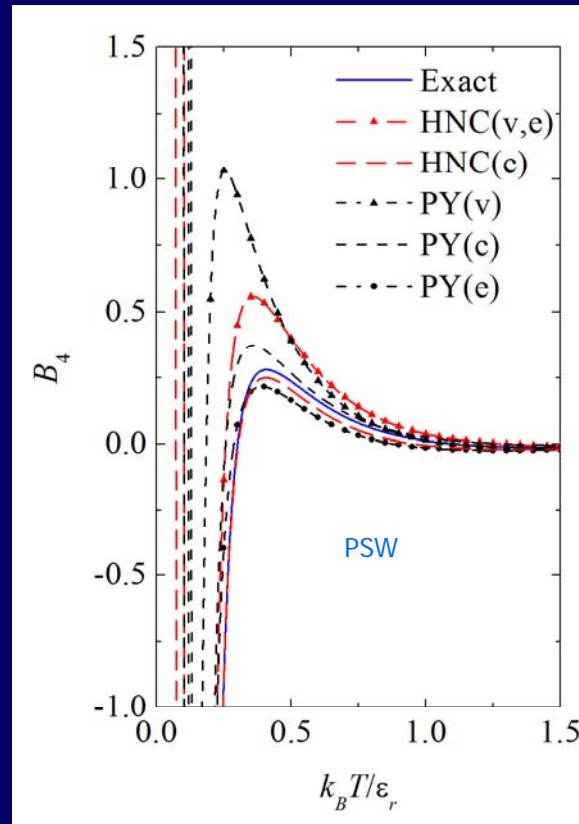
1D PSW Model: Exact low-density properties

[A.S, R. Fantoni, A. Giacometti, Phys. Rev. E **77**, 051206 (2008)]

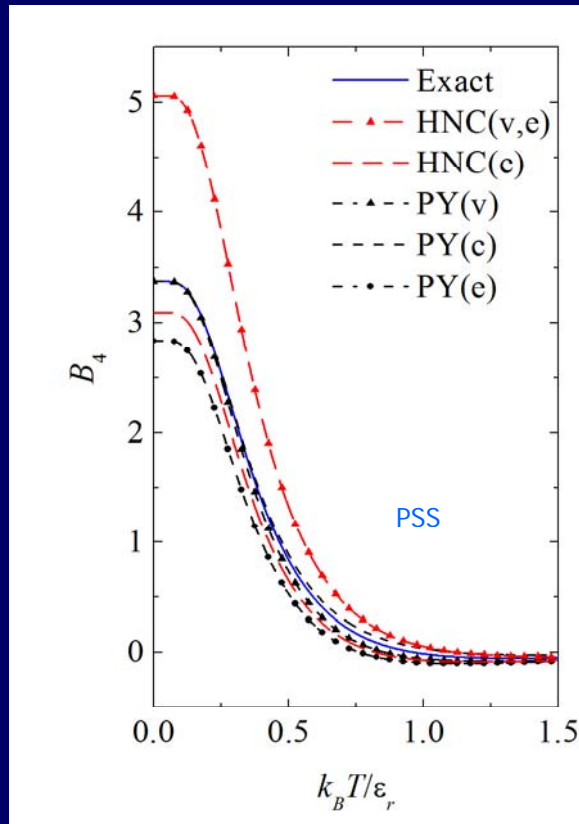


1D PSW Model: Exact low-density properties

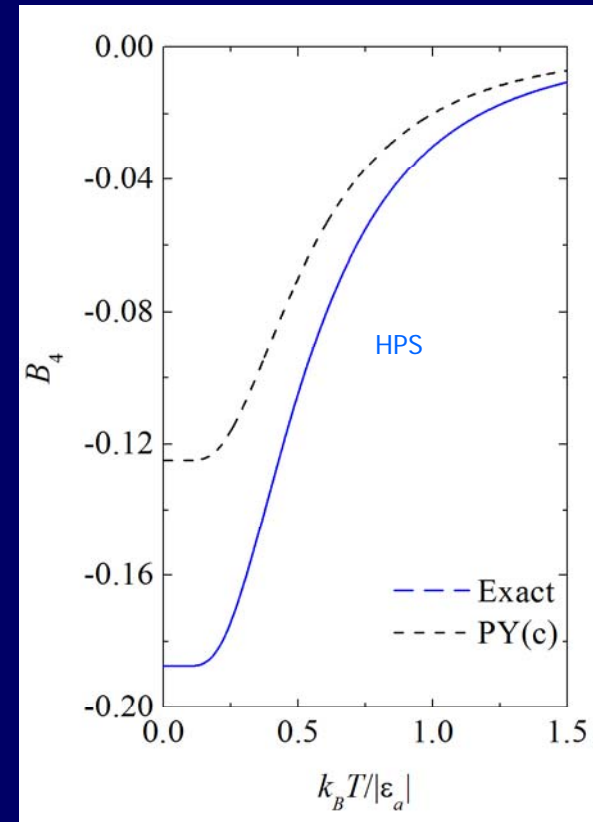
[A.S, R. Fantoni, A. Giacometti, Phys. Rev. E **77**, 051206 (2008)]



$$\epsilon_a = \frac{\epsilon_r}{4}, \quad \Delta = 0.5$$



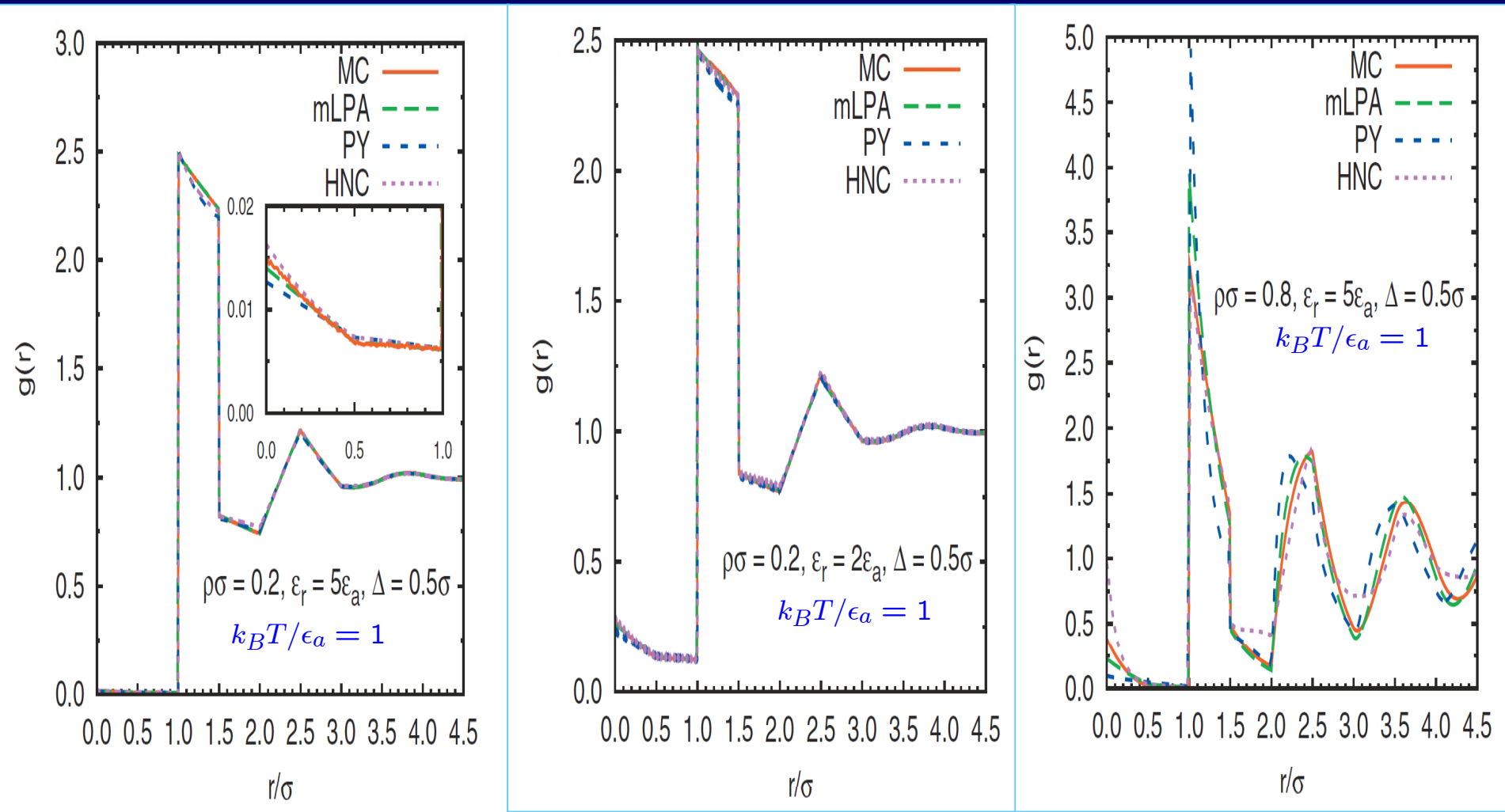
$$\epsilon_a = -\frac{\epsilon_r}{2}, \quad \Delta = 0.5$$



$$\epsilon_r = 0, \quad \epsilon_a < 0, \quad \Delta = 0.5$$

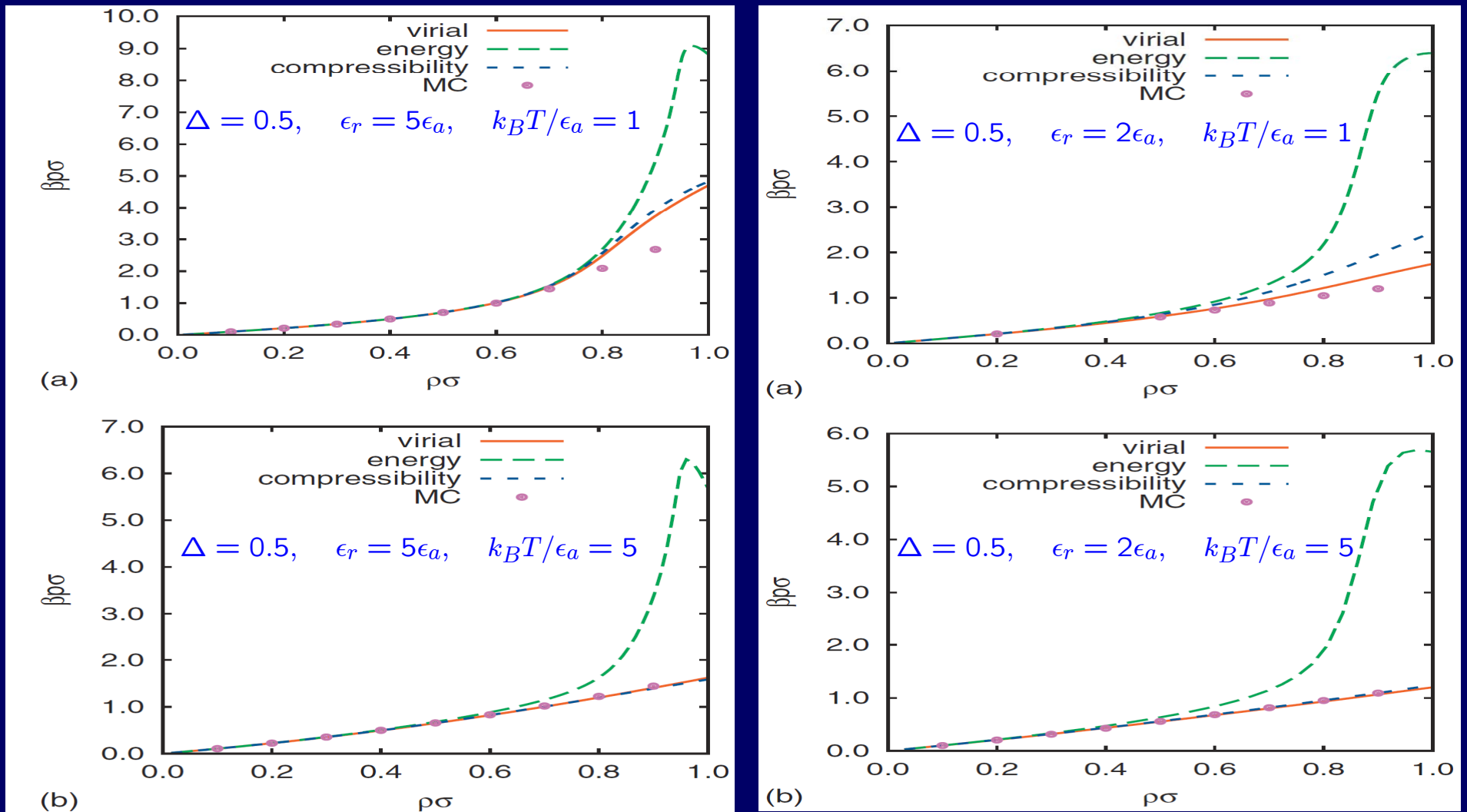
1D PSW Model: Low-penetrability approximation (LPA)

[R. Fantoni, A. Giacometti, Al. Malijevský, A.S., J. Chem. Phys. **131**, 124106 (2009)]



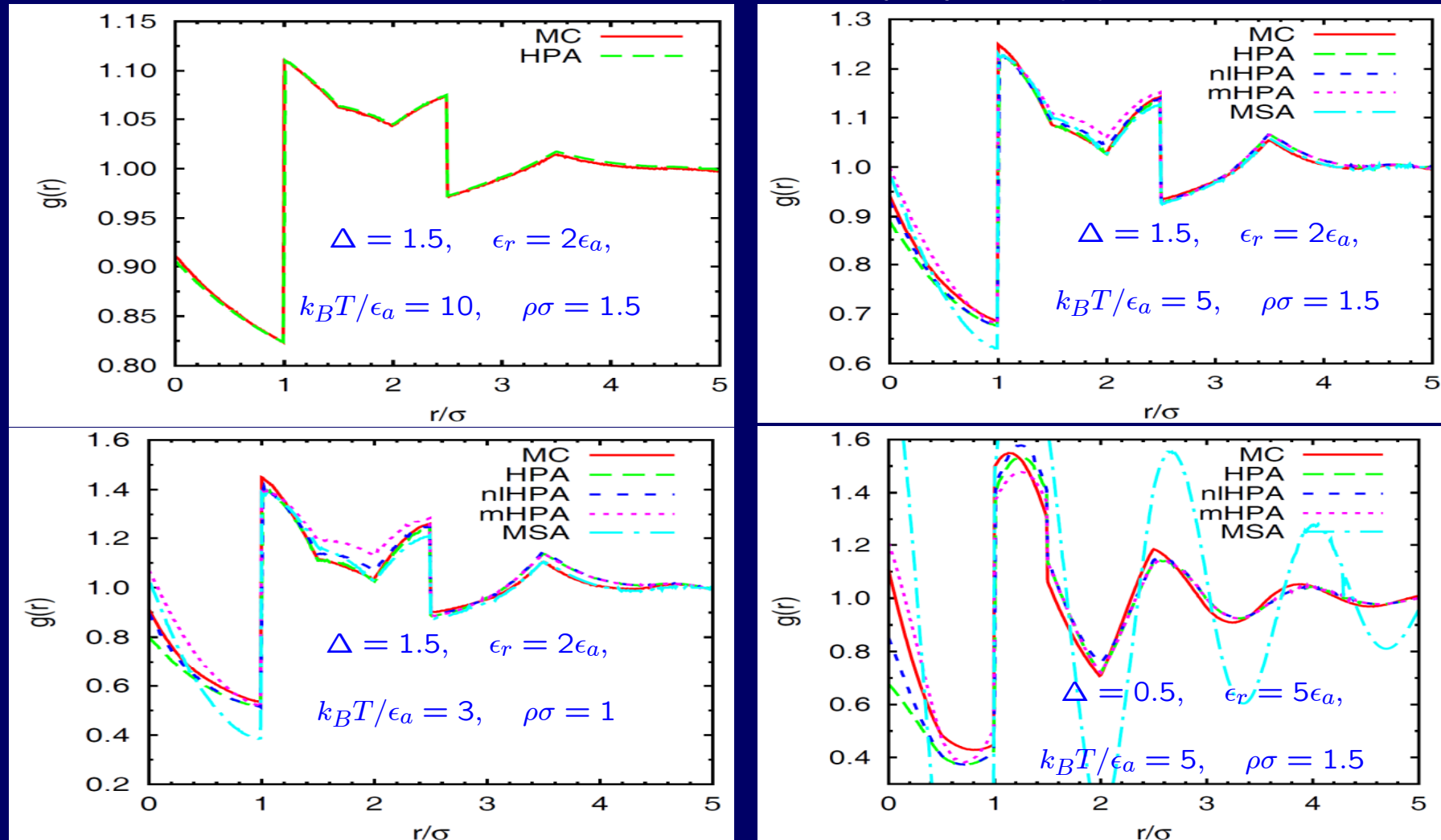
1D PSW Model: Low-penetrability approximation (LPA)

[R. Fantoni, A. Giacometti, Al. Malijevský, A.S., J. Chem. Phys. **131**, 124106 (2009)]



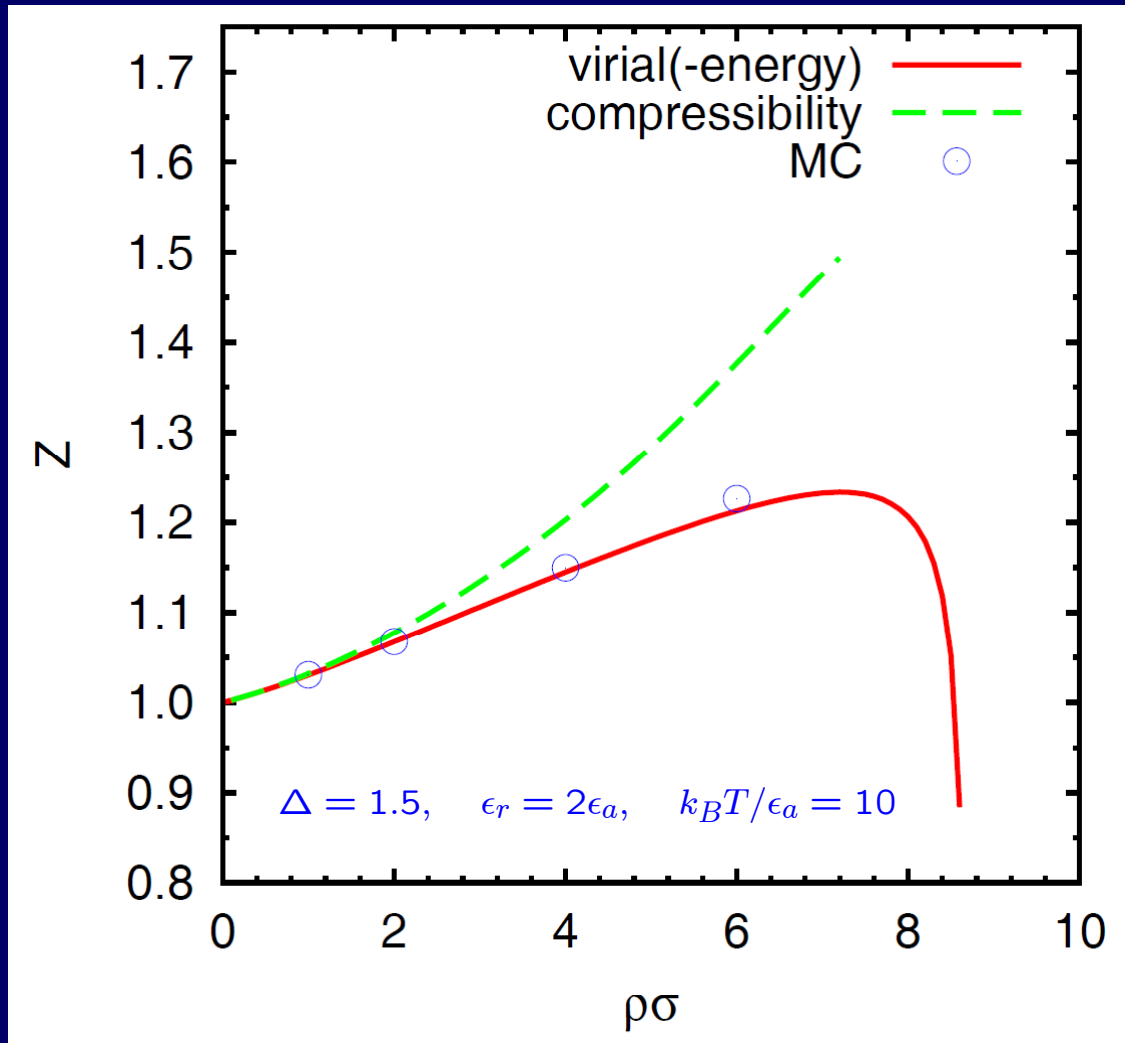
1D PSW Model: High-penetrability approximation (HPA)

[R. Fantoni, A. Giacometti, Al. Malijevský, A.S., in preparation]



1D PSW Model: High-penetrability approximation (HPA)

[R. Fantoni, A. Giacometti, Al. Malijevský, A.S., in preparation]



Conclusions?

Outline

- Effective interactions in colloidal dispersions. The penetrable-sphere (PS) model.
- Some basic concepts of statistical mechanics of equilibrium liquids.
- Exact properties of the PS fluid. Low-density limit. High-temperature, high-density limit.
- The high-penetrability and low-penetrability approximations.
- The penetrable-square-well (PSW) model.
- Transport properties of the PS model.
- Conclusions.

Transport properties of a *dilute* gas of penetrable spheres

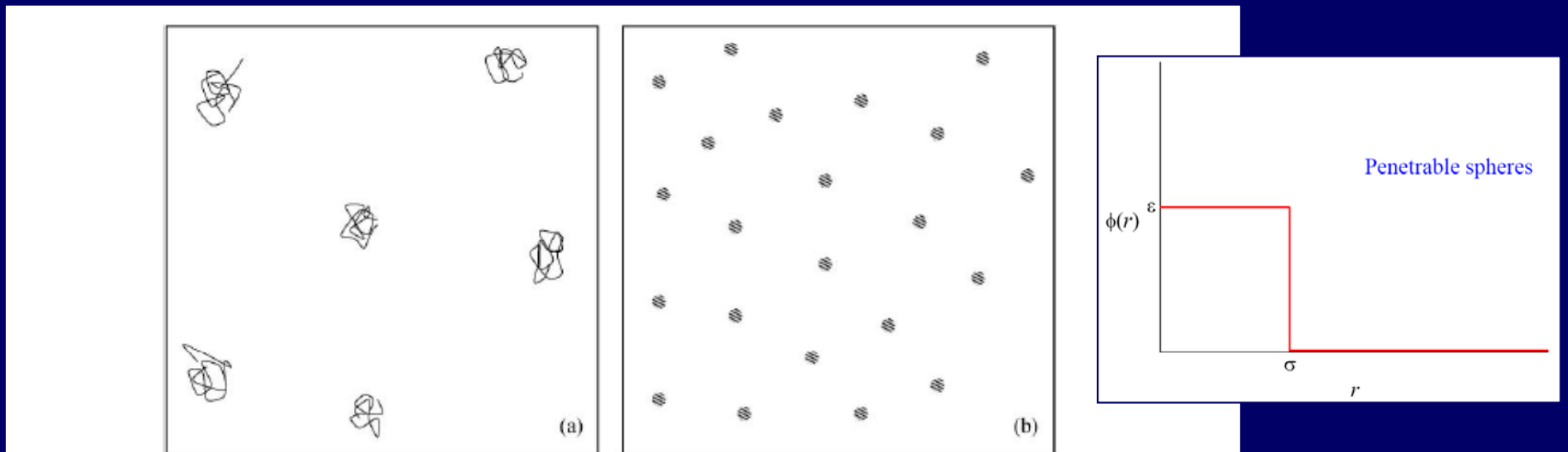


Fig. 13. A dilute polymer solution observed through two different microscopes. In (a) the microscope can resolve details above the monomer length whereas in (b) the microscope can only resolve details above the size of the chain. As a result, all length scales in (b) appear reduced with respect to those in (a) and the objects which appear as flexible chains in (a) show up as “point particles” in (b). Note that the field of view in (b) includes many more particles than in (a).

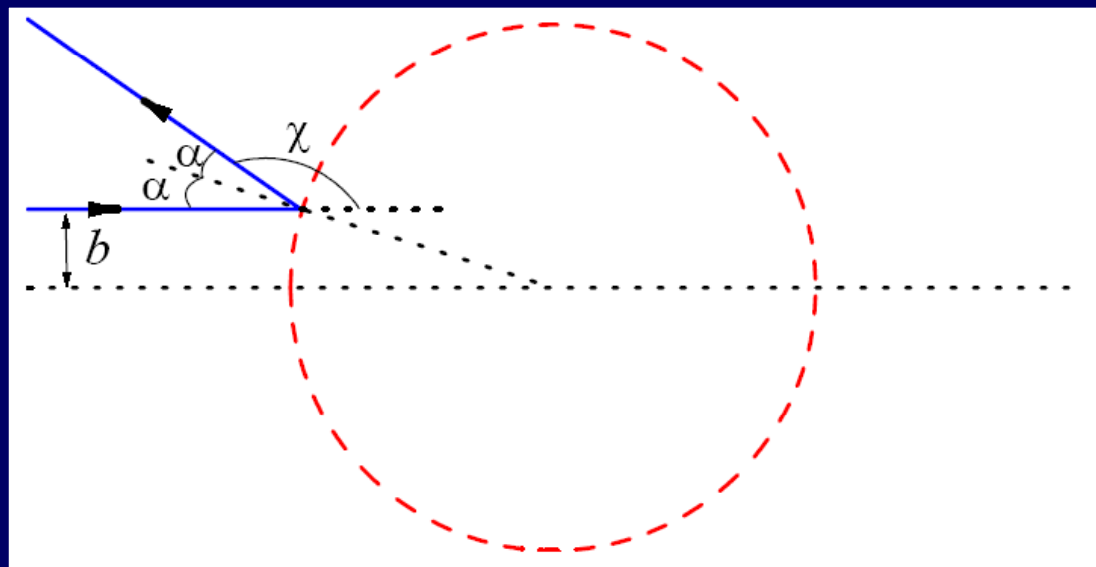
Dynamics of a collision event

Equivalent one-body problem ($\mu=m/2$, reduced mass):

$b^*=b/\sigma$ (dimensionless) impact parameter

$g^*=g/(2\varepsilon/\mu)^{1/2}$ (dimensionless) relative speed

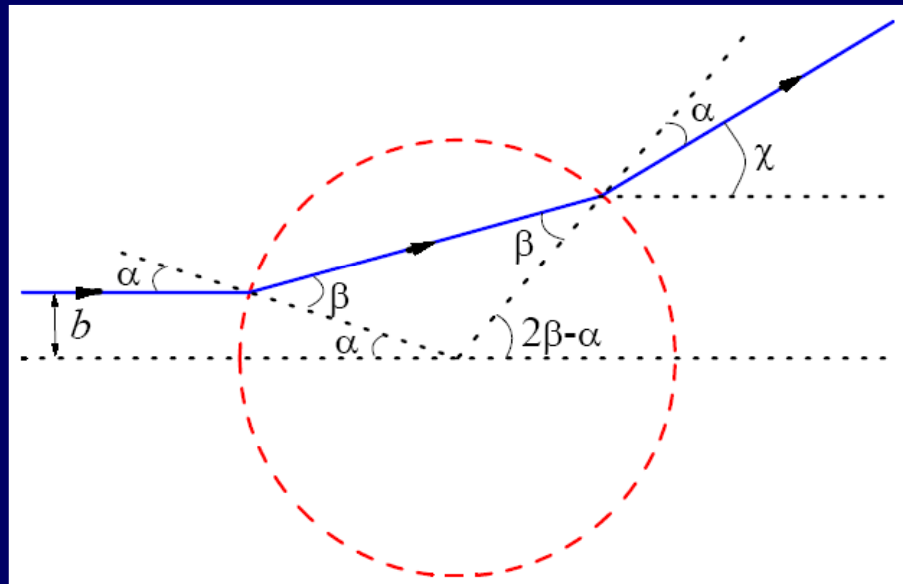
$\chi(b^*, g^*)$ scattering angle



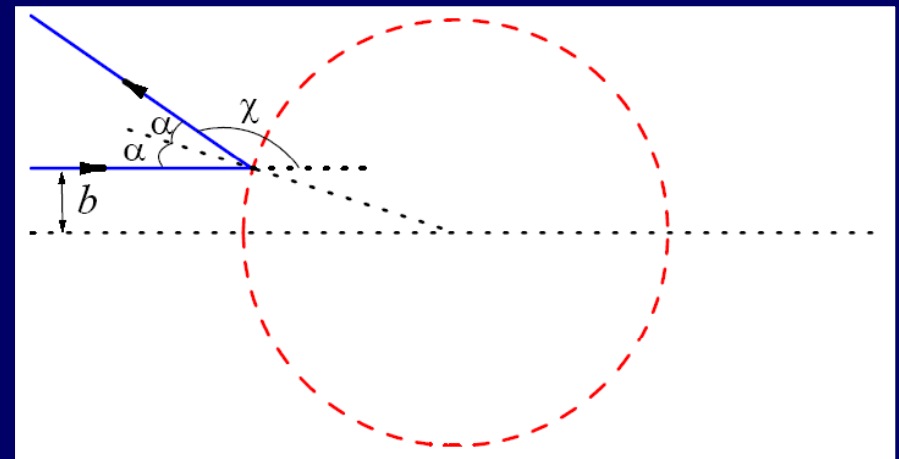
$g^*<1$: Specular reflection

$$\cos \chi(b^*, g^*) = 2b^{*2} - 1$$

$g^* > 1 \Rightarrow$ “Refraction index”: $n(g^*) = (1 - 1/g^{*2})^{1/2}$

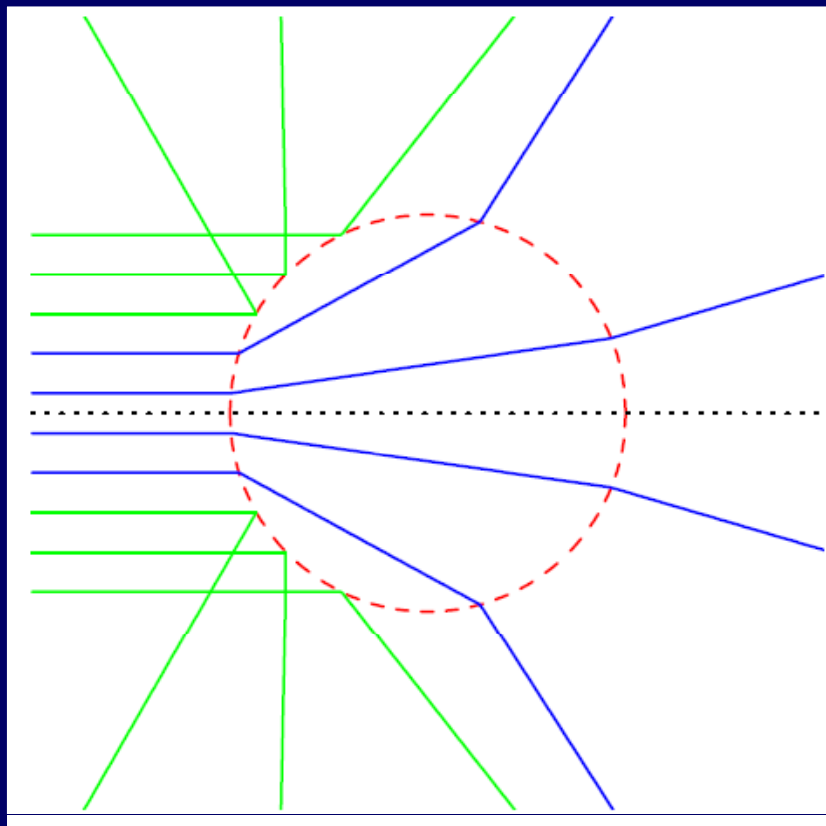


$0 \leq b^* \leq n(g^*)$
Double refraction



$n(g^*) \leq b^* \leq 1$
Total reflection

Examples of trajectories in the case $g^*=1.1$



χ is a non-monotonic function of b^*
Maximum value $\chi_{\max}(g^*) = \cos^{-1}[2n^2(g^*) - 1]$ at $b^* = n(g^*)$

Transport coefficients

$$\eta(T) = \frac{5}{8} \frac{k_B T}{\Omega_{2,2}(T)}, \quad \kappa(T) = \frac{15}{4} \frac{k_B}{m} \eta(T), \quad D(T) = \frac{3}{8} \frac{k_B T}{mn\Omega_{1,1}(T)}$$

Shear viscosity Thermal conductivity Self-diffusion

$$\Omega_{k,\ell}(T) = \sqrt{\frac{2\pi k_B T}{\mu}} \int_0^\infty dy e^{-y^2} y^{2k+3} \int_0^\infty db b \left[1 - \cos^\ell \chi(b, y\sqrt{2k_B T/\mu}) \right]$$

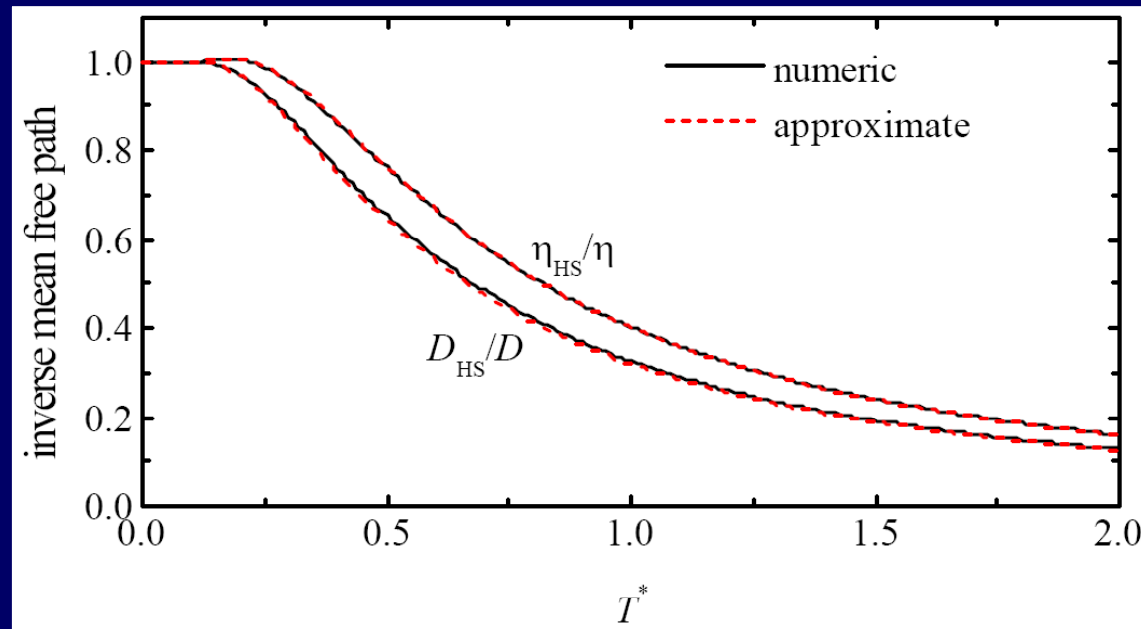
Omega-integrals

Results [A.S., AIP Conf. Proc. **762**, 276 (2005)]

$$\frac{D_{\text{HS}}(T)}{D(T)} \approx 1 - e^{-1/T^*} \left(1 + \frac{1}{T^*} \right) - \frac{\text{Ei}(-1/T^*)}{4T^{*2}}$$

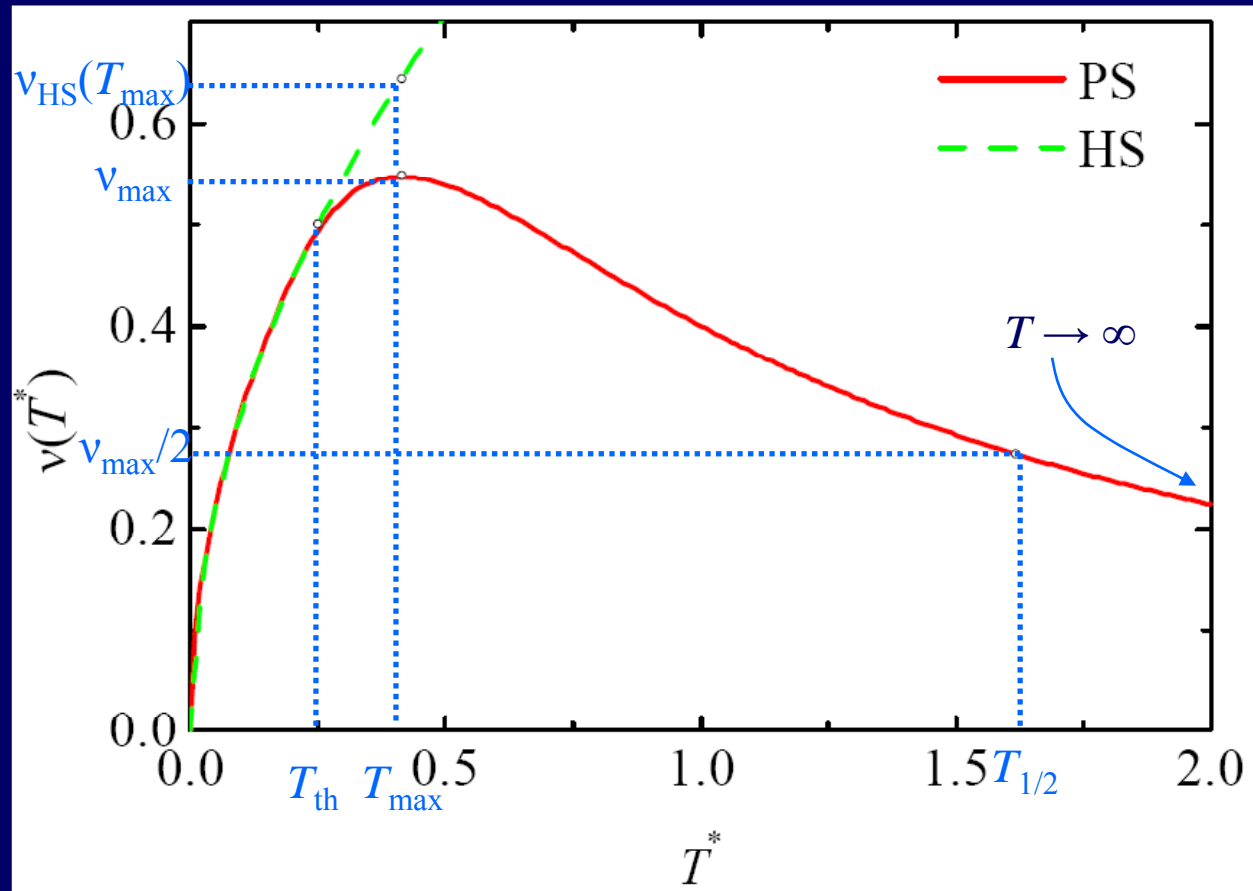
Exponential integral function

$$\frac{\eta_{\text{HS}}(T)}{\eta(T)} = \frac{\kappa_{\text{HS}}(T)}{\kappa(T)} \approx 1 - e^{-1/T^*} \left(1 + \frac{1}{T^*} - \frac{4 \ln 2 - 1}{8T^{*2}} \right) - \frac{\text{Ei}(-1/T^*)}{4T^{*2}}$$



Effective collision frequency

$$v(T^*) = nk_B T / \eta(T)$$



$$T_{\text{th}}^* = 0.25$$

$$T_{\text{max}}^* = 0.415$$

$$v_{\text{HS}}(T_{\text{max}})/v_{\text{max}} = 1.18$$

$$T_{1/2}^* = 1.619$$

$$\lim_{T^* \rightarrow \infty} v(T^*) = \frac{1}{4} T^{*-3/2} \ln T^*$$

Outline

- Effective interactions in colloidal dispersions. The penetrable-sphere (PS) model.
- Some basic concepts of statistical mechanics of equilibrium liquids.
- Exact properties of the PS fluid. Low-density limit. High-temperature, high-density limit.
- The high-penetrability and low-penetrability approximations.
- The penetrable-square-well (PSW) model.
- Transport properties of the PS model.
- Conclusions.

- The PS and PSW models allow one to describe the effective interaction in some soft matter systems, such as colloidal solutions of chain polymers.
- The models are also interesting from a theoretical point of view. They include the HS and SW fluids in the impenetrable limit, as well as the ideal gas in the infinite-temperature limit.
- The models can be *exactly* solved in the combined limit of high temperatures and densities (mean-field theory).

- By an extrapolation of those exact results, we have constructed an *analytical* theory describing high-penetrability states.
- We have also constructed a complementary *analytical* theory describing low-penetrability states.
- The transport coefficients of the low-density PS model have been derived.

Thank you for your attention!

